12-18-2004

Timing and Nature of the Deepening of the Tasmanian Gateway

Catherine E. Stickley
Cardiff University

Henk Brinkhuis
Utrecht University

Stephen A. Schellenberg
San Diego State University

Appy Sluijs
Utrecht University

Ursula Röhl
Bremen University

See next page for additional authors

Authors
Catherine E. Stickley, Henk Brinkhuis, Stephen A. Schellenberg, Appy Sluijs, Ursula Röhl, Michael Fuller, Marianne Grauert, Matthew Huber, Jeroen Warnaar, and Graham L. Williams

Timing and nature of the deepening of the Tasmanian Gateway

Catherine E. Stickley,[1] Henk Brinkhuis,[2] Stephen A. Schellenberg,[3] Appy Sluijs,[2] Ursula Röhl,[4] Michael Fuller,[5] Marianne Grauert,[6] Matthew Huber,[7] Jeroen Warnaar,[2] and Graham L. Williams[8]

Received 1 March 2004; revised 23 July 2004; accepted 20 September 2004; published 18 December 2004.

[1] Tectonic changes that produced a deep Tasmanian Gateway between Australia and Antarctica are widely invoked as the major mechanism for Antarctic cryosphere growth and Antarctic Circumpolar Current (ACC) development during the Eocene/Oligocene (E/O) transition (~34–33 Ma). Ocean Drilling Program (ODP) Leg 189 recovered near-continuous marine sedimentary records across the E/O transition interval at four sites around Tasmania. These records are largely barren of calcareous microfossils but contain a rich record of siliceous- and organic-walled marine microfossils. In this study we integrate micropaleontological, sedimentological, geochemical, and paleomagnetic data from Site 1172 (East Tasman Plateau) to identify four distinct phases (A–D) in the E/O Tasmanian Gateway deepening that are correlative among ODP Leg 189 sites. Phase A, prior to ~35.5 Ma: minor initial deepening characterized by a shallow marine prodeltaic setting with initial condensation episodes. Phase B, ~35.5–33.5 Ma: increased deepening marked by the onset of major glauconitic deposition and inception of energetic bottom-water currents. Phase C, ~33.5–30.2 Ma: further deepening to bathyal depths, with episodic erosion by increasingly energetic bottom-water currents. Phase D, <30.2 Ma: establishment of stable, open-ocean, warm-temperate, oligotrophic settings characterized by siliceous-carbonate ooze deposition. Our combined evidence indicates that this early Oligocene Tasmanian Gateway deepening initially produced an eastward flow of relatively warm surface waters from the Australo-Antarctic Gulf into the southwestern Pacific Ocean. This "proto-Leeuwin" current fundamentally differs from previous regional reconstructions of eastward flowing cool water (e.g., a "proto-ACC") during the early Oligocene and thereby represents an important new constraint for reconstructing regional- to global-scale dynamics for this major global change event. *INDEX TERMS:* 3344 Meteorology and Atmospheric Dynamics: Paleoclimatology; 3030 Marine Geology and Geophysics: Micropaleontology; 4267 Oceanography: General: Paleoceanography; 4283 Oceanography: General: Water masses; 9604 Information Related to Geologic Time: Cenozoic; *KEYWORDS:* Eocene, Oligocene transition, Tasmanian Gateway, diatoms and dinoflagellate cysts

Citation: Stickley, C. E., H. Brinkhuis, S. A. Schellenberg, A. Sluijs, U. Röhl, M. Fuller, M. Grauert, M. Huber, J. Warnaar, and G. L. Williams (2004), Timing and nature of the deepening of the Tasmanian Gateway, *Paleoceanography*, *19*, PA4027, doi:10.1029/2004PA001022.

1. Introduction

[2] The transition from a relatively warm early Cenozoic "Greenhouse" to a late Cenozoic "Icehouse" global state is traditionally linked to the opening of Southern Ocean gateways [*Kennett et al.*, 1975; *Murphy and Kennett*, 1986; *Zachos et al.*, 1996], with the Tasmanian Gateway opening associated with the onset of Antarctic glaciation at the end of the Eocene (~33.5 Ma) and the Drake Passage opening reported to occur in the early or late Oligocene [*Lawver and Gahagan*, 2003; *Barker*, 2001]. The "Tasmanian Gateway Hypothesis" suggests that the onset of Antarctic glaciation and associated global cooling across the Eocene-Oligocene (E/O) transition resulted from the thermal isolation of continental Antarctica from relatively warm equatorial-sourced limbs of surface current gyres as a consequence of the opening of the Tasmanian Gateway between Australia and Antarctica [*Kennett et al.*, 1975; *Murphy and Kennett*, 1986; *Exon et al.*, 2001]. Previous drilling in the Tasman Sea region (e.g., Deep Sea Drilling Project (DSDP) Leg 29) contributed to the development of the Tasmanian Gateway Hypothesis but was of insufficient recovery to fully test this hypothesis. Recent drilling during Ocean Drilling Program (ODP) Leg 189 (Sites 1168–1172; Figure 1) provided near-continuous core recovery and allows detailed reconstruction

[1]School of Earth, Ocean and Planetary Sciences, Cardiff University, Cardiff, UK.
[2]Laboratory of Palaeobotany and Palynology, Utrecht University, Utrecht, Netherlands.
[3]Department of Geological Sciences, San Diego State University, San Diego, California, USA.
[4]Research Center for Ocean Margins, Department of Geosciences, Bremen University, Bremen, Germany.
[5]Hawaii Institute of Geophysics and Planetology, University of Hawaii at Manoa, Honolulu, Hawaii, USA.
[6]Department of Geography, University of Copenhagen, Copenhagen, Denmark.
[7]Earth and Atmospheric Science, Purdue University, West Lafayette, Indiana, USA.
[8]Geological Survey of Canada (Atlantic), Bedford Institute of Oceanography, Dartmouth, Nova Scotia, Canada.

0883-8305/04/2004PA001022

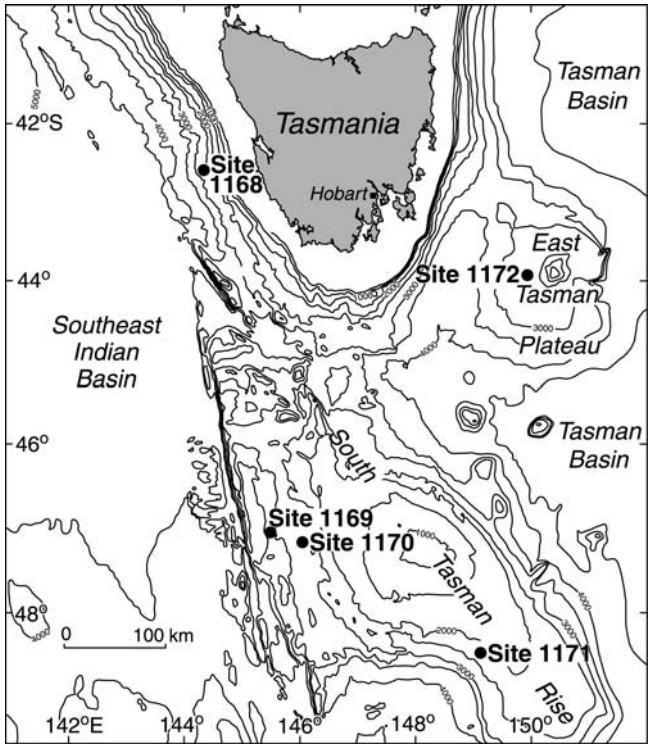

Figure 1. ODP Leg 189 drill sites and bathymetric map of the Tasmanian Seaway.

of the timing, nature and climatic effects of the opening of the Tasmanian Gateway.

[3] Sediments spanning the E/O transition were recovered at four sites of ODP Leg 189, with those at Site 1172 being the most complete [*Exon et al.*, 2001]. The E/O interval is essentially barren of calcareous microfossils at all sites, impeding traditional biostratigraphic assessment. However, siliceous and organic-walled phytoplankton remains are abundant, allowing detailed age assessment and paleoenvironmental reconstruction. Here we present diatom and organic-walled dinoflagellate cyst (dinocyst) analyses with geochemical (i.e., bulk weight percent carbonate, weight percent organic carbon, and bulk carbonate $\delta^{18}O$ and $\delta^{13}C$), sedimentological (i.e., grain size) and physical property (i.e., paleomagnetic) data for the E/O interval at Site 1172. We focus on (1) establishing a rigorous biochronological framework and (2) determining the nature of the environmental changes associated with the opening of the Tasmanian Gateway. This integrated approach provides a means to date and reconstruct events associated with the separation of Australia and Antarctica, and thereby to evaluate the potential role of this tectonic event in mid-Paleogene global climate change.

2. Materials and Methods

[4] ODP Leg 189 drill sites (Figure 1), at present located in water depths of 2475 to 3579 m, rest on submerged continental blocks that were part of the "Tasmanian Land Bridge" (~65–70°S paleolatitude), a partly submerged promontory that effectively blocked the eastern end of the progressively widening Australo-Antarctic Gulf (AAG) until the latest Eocene. The recovered sedimentary sequences are entirely marine, with substantial terrestrial input until the earliest Oligocene, and contain a wealth of microfossil assemblages that record paleoenvironmental conditions from the latest Cretaceous (~70 Ma) onward [*Exon et al.*, 2001]. Shipboard studies indicate that the E/O transition interval was recovered at four sites: Site 1168 (West Tasmanian Margin), 1170 and 1171 (South Tasman Rise) and 1172 (East Tasman Plateau).

[5] Shipboard data from all four sites indicate a succession of three distinct lithological units through the middle Eocene to lower Oligocene interval [*Exon et al.*, 2001]. Broadly, these units are (1) middle Eocene to lower upper Eocene, brown-gray, shallow marine, organic-rich clay and siltstones that formed under relatively high sediment accumulation rates; (2) middle upper Eocene to lowermost Oligocene, green, shallow marine glauconite-rich silt and sandstones, which appear highly condensed; and (3) lower Oligocene and younger deep marine, white, siliceous-rich, carbonate ooze that formed under moderate sediment accumulation rates. The glauconite or "greensand" unit, interpreted to reflect marked subsidence and opening of the Tasmanian Gateway, is essentially barren of calcareous microfossils at Sites 1170, 1171, and 1172 [*Exon et al.*, 2001]. However, diatoms are abundant and well-preserved throughout, and dinocysts are highly abundant through the lower half of the unit. Core recovery across the E/O transition interval was most complete at Site 1172 (in Holes 1172A and 1172D). Moreover, both initial and postcruise studies demonstrate that the microfossil record at Site 1172 is not only exceptionally rich, but that it is representative of the western and south-central Tasmanian region [e.g., *Brinkhuis et al.*, 2003b; *Sluijs et al.*, 2003]. We therefore selected this site (in particular Hole 1172A) for the more detailed integrated study presented here.

[6] The E/O lithological sequence of Hole 1172A (summarized in Figure 2a) is as follows: Core 189-1172A-41X through the upper third of section 5 of Core 189-1172A-39X (383.4–361.12 mbsf) comprise siliciclastic, greenish-gray to dark greenish gray, and dark brownish gray, diatom- and dinocyst-bearing claystone to very dark brown and very dark gray-brown diatomaceous claystone (local subunit IIIA; *Shipboard Scientific Party* [2001a]). This basal unit is overlain by ~5 m of essentially diatomaceous glauconitic siltstone or "greensand" (local unit II) in the upper third of section 5 through the lowermost part of section 1 of Core 189-1172A-39X (361.12 to 355.80 mbsf). The greensand is relatively thin, but contains a complex succession of sediments (see *Shipboard Scientific Party* [2001a] for detailed description) and is commonly bioturbated. Of particular note within the greensand is a marked increase in glauconite content at ~360.6 mbsf (base of section 4), and a distinct lithological break at ~357.39 mbsf that divides the purer glauconitic sands below from an overlying ~2 m thick, light greenish-gray "transitional chalk" interval of glauconite-, diatom-, and clay-bearing nannofossil chalk (ooze). Above this transitional unit (above ~355.8 mbsf) is white, foraminiferal-bearing, siliceous nannofossil chalk (ooze) and

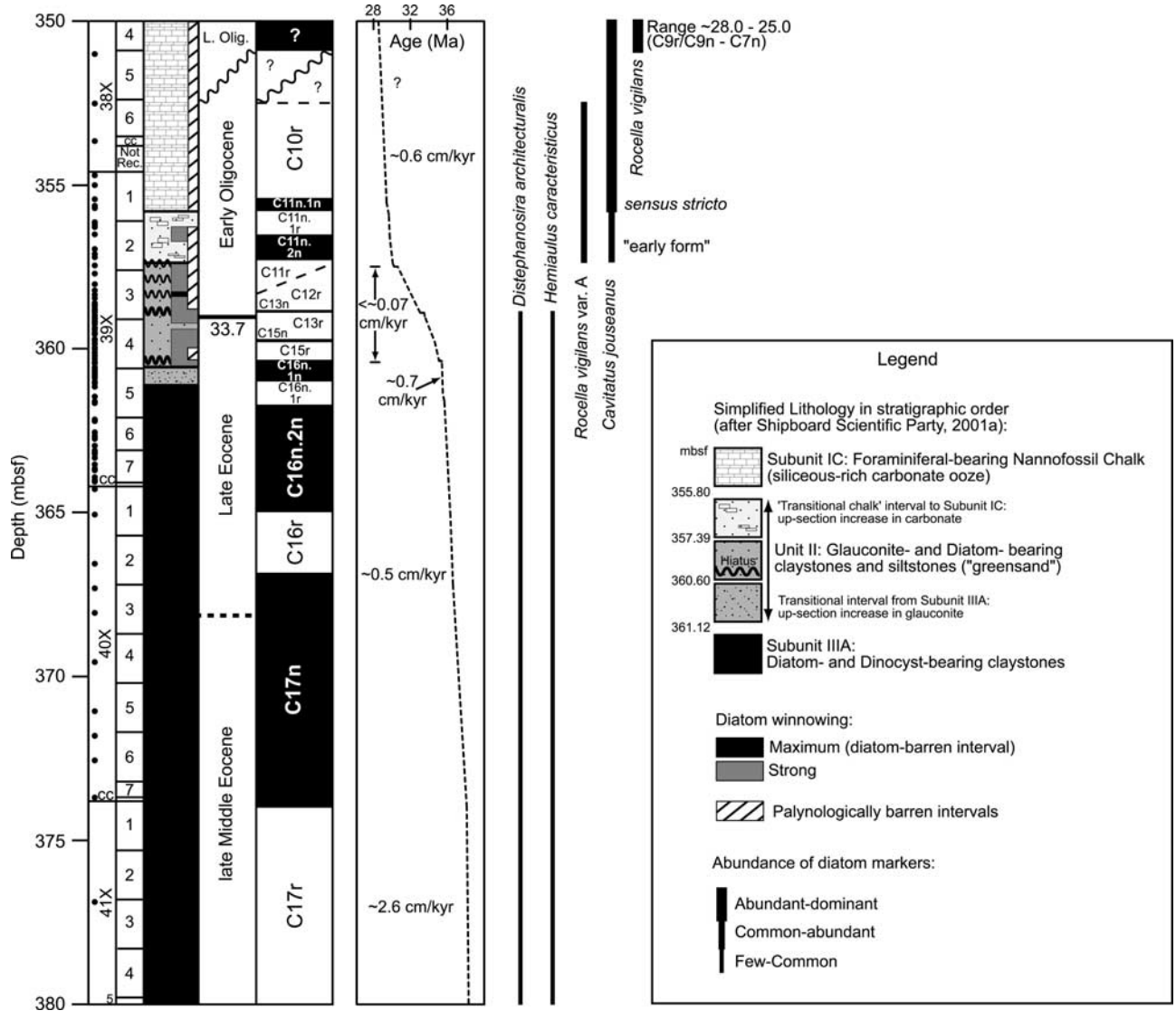

Figure 2a. Age model and simplified lithostratigraphy of Hole 1172A. Lithology, magnetostratigraphy, chronostratigraphy, age-depth plot, and ranges of marker diatoms discussed in the text, through Cores 189-1172A-38X through -41X. Core sections and sample points for diatom and organic-walled dinoflagellate cyst (dinocyst) analysis (black dots) are indicated. Sequence condensation through the critical interval is highlighted by the age-depth plot (average linear sedimentation rates indicated).

clay-bearing, nannofossil chalk (ooze; local subunit IC), which contain a considerable amount of biogenic silica (largely diatoms with relatively minor amounts of Ebridians, silicoflagellates, chrysophyte cysts and radiolarians). Diatoms are common to abundant throughout the studied interval (~380–350 mbsf) and dinocysts are abundant from local subunit IIIA through to the lower part of the greensand unit (local unit II; ~380–359 mbsf).

[7] Shipboard biostratigraphic studies indicated that the E/O transition interval occurs within the greensand unit of Core 189-1172A-39X, and most likely within sections 3–5 [*Shipboard Scientific Party*, 2001a]. Therefore we analyzed diatom and palynomorph assemblages in Cores 189-1172A-41X through -38X at an average sampling resolution of ~20–50 cm, and increased this sampling resolution to 1–4 cm for the upper part of section 5 through the upper part of section 3 of Core 189-1172A-39X (n = 92, 23 analyzed for both diatoms and palynomorphs). Micropaleontological processing techniques followed standard methods outlined by *Shipboard Scientific Party* [2001b]. We focused exclusively on Core 189-1172A-39X for all other analyses; geochemical analyses were conducted at a sampling resolution of ~8.5 cm (n = 110) throughout the Core 39X, and grain size analysis was conducted at a sampling resolution of 4–6 cm (n = 110) on sections 2 through 5.

2.1. Diatom Analysis

[8] Diatom processing and analysis were carried out in the Environmental Change Research Centre (University College London), and Lamont-Doherty Earth Observatory

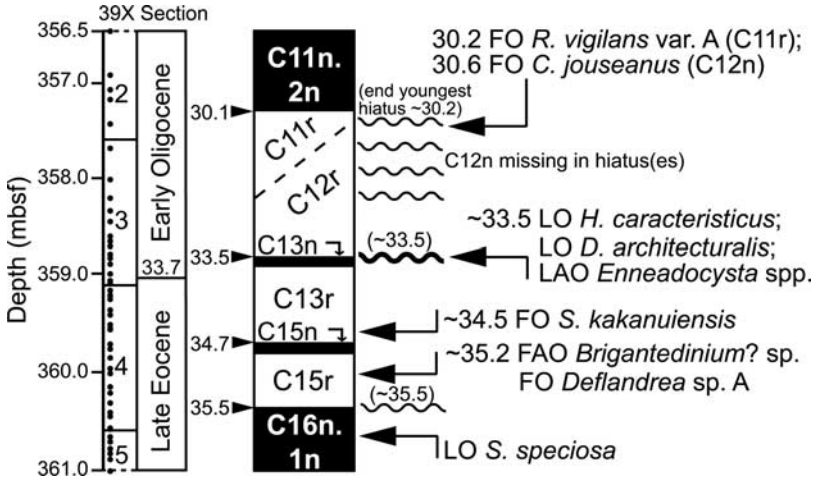

Figure 2b. Detailed age model across the Eocene/Oligocene transition interval within Core 189-1172A-39X. Diatom and dinocyst datums are indicated against the magnetostratigraphic column. F(A)O, first (abundant) occurrence; L(A)O, last (abundant) occurrence. Sample points for dinocyst-diatom analysis indicated within the core/section. Hiatuses indicated by wavy lines. All ages are indicated in Ma and depths in meters below seafloor (mbsf). See text for generic names where not indicated.

(Columbia University). For quantitative diatom analysis, 1 ml of divinylbenzene microspheres (concentration 9.735 $\times$ 10^6 spheres/ml) was added to each of the digested samples prior to slide preparation, following the methods of *Battarbee and Kneen* [1982] and *Battarbee* [1986]. Standard counting procedures [e.g., *Schrader and Gersonde*, 1978] were followed. The full count data, absolute abundance values, methodologies, range charts and diatom plates are provided by C. E. Stickley (manuscript in preparation, 2004). We provide semiquantitative data and ranges for only the biostratigraphical marker diatoms discussed in this paper (Figures 2a and 2b). Owing to the occurrence of a number of undescribed taxa, it was not always possible to identify diatoms below the generic level. Formal descriptions of new taxa are the subject of another contribution. Diatoms were tallied in the following groups: (1) benthic neritic (or tychopelagic), e.g., species of the genera *Actinoptychus*, *Arachnoidiscus*, *Biddulphia* (and related taxa), *Cocconeis*, *Diploneis*, *Hyalosira*, *Melosira*, *Paralia*, *Podosira*, *Pseudopodosira*; (2) "offshore" (oceanic, holoplanktonic), e.g., species of the genera *Actinocyclus*, *Asterolampra*, *Asteromphalus*, *Azpeitia*, *Cavitatus*, *Cestodiscus*, *Coscinodiscus*, *Eurossia*(?), *Proboscia*, *Rhizosolenia*, *Rocella*, *Rouxia*, *Sceptroneis*, *Sheshukovia*, *Stellarima*, *Triceratium*, *Trinacria*(?); (3) nutrient indicators, i.e., resting spores of the genera *Chaetoceros*, *Dicladia*, *Goniothecium*, *Pterotheca* and *Xanthiopyxis*; (4) Antarctic "endemic" (see below), i.e., *Arachnoidiscus oamaruensis*, *Cestodiscus antarcticus*, *Distephanosira architecturalis* (?early middle Eocene), *Hemiaulus caracteristicus* (middle Eocene), *H. incisus*, *H. stilwelli*, *Stictodiscus hardmanianus*(?) all undescribed diatoms in this study (see C. E. Stickley, manuscript in preparation, 2004), as well as the following informally treated diatoms by *Harwood and Bohaty* [2001]: ?*Biddulphia* sp. A, *Sheshukovia* sp. A and B, *Sphynctolethus* sp. A., *Stephanopyxis* sp. ?B, E and F; (5) cosmopolitan planktonic, including importantly *Cavitatus jouseanus*, *Coscinodiscus marginatus*, *Coscinodiscus radiatus*, *Distephanosira architecturalis* (late middle to late Eocene), *Rocella praenitida*, *R. vigilans* vars A and B, and all species of the genera *Triceratium* and *Trinacria*.

[9] Diatom preservation, with respect to the relative proportions of larger robust versus smaller weakly silicified valves, was also recorded. Relative abundance peaks in the former are interpreted as a proxy for winnowing (Figure 2a) in the Eocene interval since the shallow water depths likely resulted in little dissolution. Major floral patterns are depicted in Figures 3 and 4.

2.2. Palynological Analysis

[10] Palynological methods and the data presented here are discussed in detail by *Sluijs et al.* [2003]. Palynological processing and analysis were carried out at the Laboratory of Palaeobotany and Palynology at Utrecht University. Palynological slides were counted for palynomorphs generally, and for dinocysts in detail. Dinocyst taxonomy follows *Williams et al.* [1998] and all material is curated at the Laboratory of Palaeobotany and Palynology, Botanical Palaeoecology, Utrecht University, Netherlands. Palynological count data are provided by *Sluijs et al.* [2003] and major faunal patterns are depicted in Figures 3 and 4.

2.3. Geochemical Analyses

[11] Geochemical analyses were conducted at the Institute of Marine Sciences at the University of California, Santa Cruz. Bulk sediment splits from core samples were freeze-dried, crushed to <150 μm grain size, and analyzed for weight percent carbonate (wt % $CaCO_3$), weight percent total organic carbon (wt % TOC), and bulk carbonate $\delta^{13}C$ and $\delta^{18}O$ values. Wt % $CaCO_3$ was determined by 2N H_2SO_4 acidification of 20.00 to 50.00 mg of bulk sediment and coulometric measurement of the mg C in evolved CO_2 gas. Analytical precision was better than ±1.3% (one relative standard deviation) based on 16 intrarun analyses

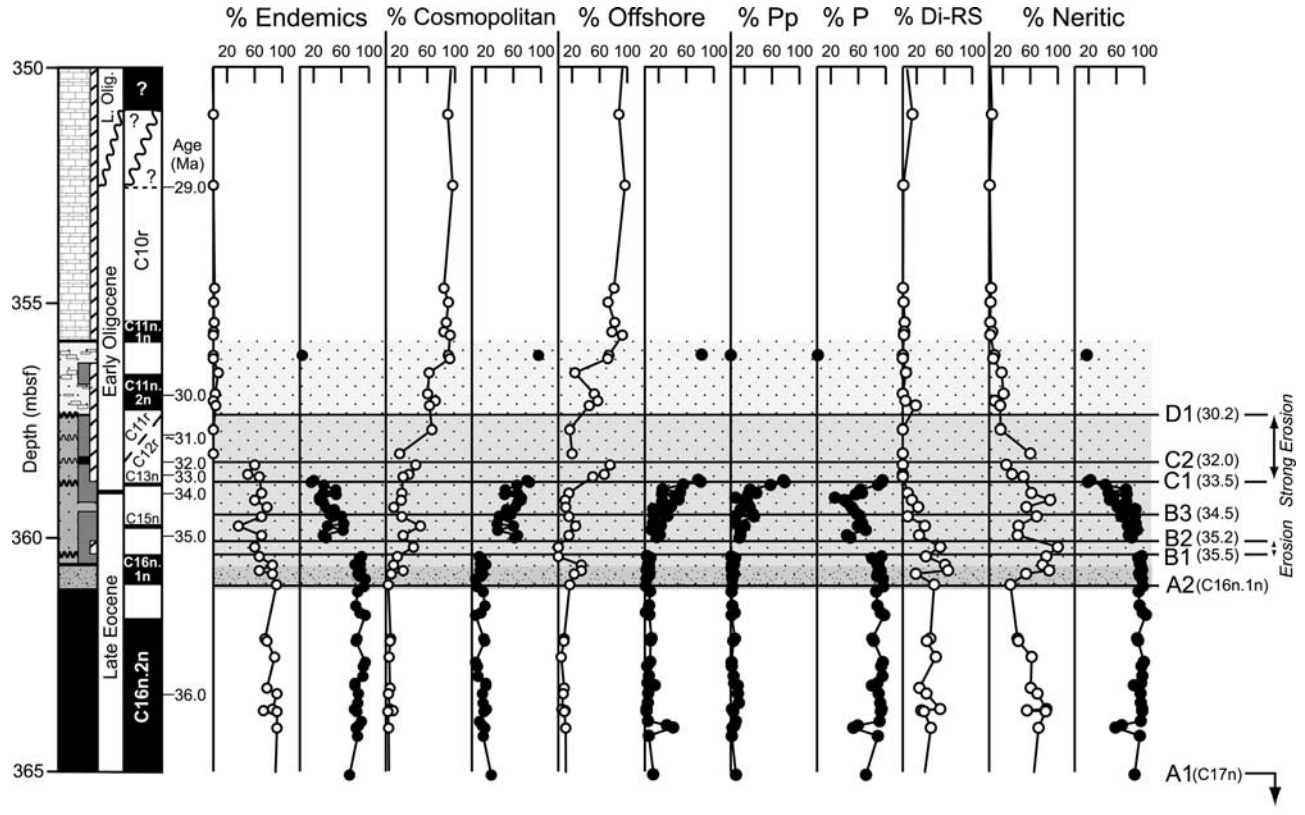

Figure 3. Diatom and organic-walled dinoflagellate cyst (dinocyst) relative abundance changes through the Eocene/Oligocene transition interval of Hole 1172A. Open circles, diatom data; closed circles, dinocyst data; Pp, Protoperidinioid dinocysts; P, Peridinioid dinocysts; Di-RS, diatom resting spores. Breaks in the data imply barren samples. Lithological changes over the interval are indicated through the data (see Figure 2a for legend). Diatoms: Relative abundance diatom data exclude all heavily silicified dominant taxa (*Stephanopyxis turris*, *S. grunowii* and all species of *Pyxilla*). Cosmopolitan diatoms refer to planktonic oceanics only. Diatom resting spores (e.g., *Chaetoceros*, *Dicladia*, *Pterotheca*, *Xanthiopyxis* + associated taxa) are nutrient indicators. Neritic diatoms refer to benthic neritic diatoms only. Dinocysts: Both endemic and bipolar dinocysts are indicated in the relevant percent endemic curve. Offshore dinocysts are oceanics + *Spiniferites* + *Enneadocysta*. Protoperidinioids (heterotrophs) notably include *Brigantedinium* (oceanic). Peridinioids are presumed heterotrophic. Neritic dinocysts = neritic and restricted taxa. The evolutionary phases discussed in the text are marked by lines A1–D1 (ages indicated in parenthesis). Line A1: Initial moderate deepening during Chron C17n. Line A2: Brief return to moderate sedimentation rates during Subchron C16n.1n. Line B1: ~35.5 Ma, first deepening step; inception of energetic bottom currents; brief palynology break. Line B2: ~35.2 Ma, FAO *Brigantedinium*? sp.; ~end first erosional event; ~installment of oceanic upwelling. Line B3: ~34.5 Ma, FO *S. kakanuiensis*; first west-to-east surface water connection between AAG and Pacific sites (same water mass). Line C1: ~33.5 Ma, further deepening; intensification of energetic bottom currents; end palynology. Line C2: ~32 Ma, end "endemics"; hiatus, followed by inception of oceanic, oligotrophic, warm-temperate conditions. Line D1: ~30.2Ma, end major erosion; start of siliceous-rich carbonate ooze deposition with cosmopolitan phytoplankton.

of a pure $CaCO_3$ standard, while sample reproducibility was better than ±1.5% (one relative standard deviation) for wt % $CaCO_3$ values greater than 1 wt % (based on 6 replicate analyses of 3 samples) and better than ±6.7% (one relative standard deviation) for wt % $CaCO_3$ values less than 1 wt % (based on 6 replicate analyses of 3 samples). Wt % TOC for each sample interval was calculated by subtracting the wt % $CaCO_3$ value from the total wt % carbon value as determined by roasting 20.00 to 50.00 mg splits of bulk sediment at 950°C and coulometric measurement of the mg C in evolved CO_2 gas. Wt % TOC sample reproducibility was better than ±9.6% (one relative standard deviation with propagated error based on 6 replicate analyses of 6 sample pairs). Oxygen and carbon stable isotope values were determined by isotope ratio mass spectrometry (IRMS) as follows: Bulk sediment samples of 6–15 mg were first roasted under vacuum at 350°C for one hour to remove organic carbon. Bulk $CaCO_3$ within the bulk samples was

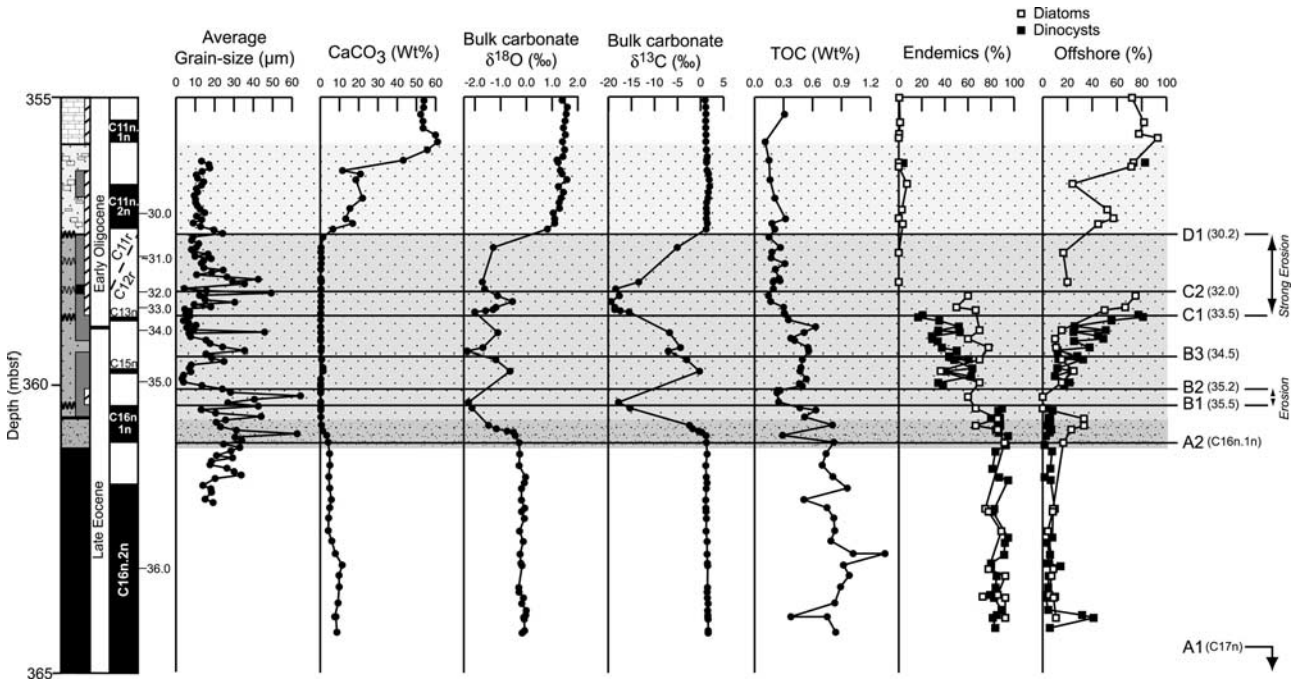

Figure 4. Average grain size, whole core carbonate ($CaCO_3$), bulk carbonate $\delta^{18}O$ and $\delta^{13}C$ and total organic carbon (TOC) through the Eocene/Oligocene transition interval of Hole 1172A compared with endemic and offshore phytoplankton abundance. Open squares, diatom data; closed squares, organic-walled dinoflagellate cyst (dinocyst) data. Lithological changes over the interval are indicated through the data. See Figure 2a for legend. See Figure 3 caption for significance of lines A1–D1.

converted to CO_2 by acidification in 100% H_3PO_4 at 90°C using an automatic carbonate device with common acid bath. Evolved CO_2 was analyzed for $\delta^{18}O$ and $\delta^{13}C$ using a FISONS Optima mass spectrometer with values reported relative to the VPDB standard. Long-term analytical precision based on NBS-19 and in-house Carrara Marble carbonate standards averaged better than ±0.06 (one standard deviation) and ±0.04 (one standard deviation) for $\delta^{18}O$ and $\delta^{18}C$, respectively. Geochemical data are presented in Figure 4, and a table of these data are available as an electric supplement.[1]

2.4. Grain-Size Analysis

[12] Grain-size analysis was conducted at the Institute of Geography, University of Copenhagen. Each sample was treated with 3 M HCl to dissolve carbonate and rinsed with deionized water. Samples were then boiled at 60°C in H_2O_2 (30%) for several hours to oxidize all organic matter and rinsed twice with deionized water. Samples were then boiled at 90°C in 0.3 M NaOH for 3 hours to maximize dissolution of biogenic opal. Finally, samples were rinsed 3–4 times with deionized water. Prior to grain-size analysis, samples received 1 ml of 0.002M sodium hexametaphosphate ($Na_4P_2O_7 \times 10H_2O$) and were sonicated for 4 min to disaggregate sediment grains. Grain-size distributions were determined by a Mastersizer 2000 (Malvern Instruments) using laser diffraction methods [*Agrawal et al.*, 1991]. Each sample was analyzed six times and the instrument cleaned 3 times over the entire run of 110 samples. Grain-size data are presented in Figure 4, and a table of these data are available as an electric supplement. While clay- and silt-sized grains typically predominate the nonbiogenic record, distinctive sand-sized populations are clearly present to varying degrees and drive the major shifts in mean grain size.

2.5. Magnetostratigraphic Analysis

[13] Site 1172 magnetostratigraphy was initially developed from interpretation of the results obtained from the shipboard pass through cryogenic magnetometer [*Shipboard Scientific Party*, 2001a], and subsequently refined by paleomagnetic determinations on discrete samples [*Fuller and Touchard*, 2004; *Stickley et al.*, 2004]. Polarity chron assignments were based upon biostratigraphic constraints (see diatom events below; *Stickley et al.* [2004]) coupled with the distinctive pattern of normal- and reversed-polarity zones. Magnetostratigraphic interpretations are presented in Figures 2a–4.

3. Age Model and Sedimentation Rates

[14] Shipboard biostratigraphic and paleomagnetic data allowed a provisional age assignment of late middle Eocene (Chron C17r) to late early Oligocene (Chron C10r) to the studied interval (Cores 189-1172A-41X to -38X; ~377–350 mbsf) [*Shipboard Scientific Party*, 2001a]. Here we refine this age model through higher-resolution diatom and dinocyst biostratigraphy and postcruise paleomagnetic

[1] Auxiliary material is available at ftp://ftp.agu.org/apend/pa/2004PA001022.

determinations (in part also constrained by the cyclostratigraphic study by *Röhl et al.* [2004]). Combined results are presented below and summarized in Figures 2a and 2b. All biomagnetostratigraphic datums are assigned absolute ages using the geochronological timescale of *Berggren et al.* [1995].

3.1. Magnetostratigraphy

[15] Magnetic polarity zones are fairly well-defined in ODP Hole 1172A [*Fuller and Touchard*, 2004; *Stickley et al.*, 2004]. In the studied interval, most late Eocene to early Oligocene chrons are present with the notable exception of C12n, an interpretation consistent with diatom biostratigraphy (see below; Figures 2a–4). Within the greensand unit, two short normal polarity zones, occurring at 359.8–359.7 mbsf and 358.9–358.8 mbsf, are interpreted as C15n and C13n, respectively, based on their stratigraphic position and relative biostratigraphic datums. The identification of these specific chrons greatly facilitated age assignment for the broader boundary interval. *Röhl et al.* [2004] provides details on the magnetostratigraphic identification of Chrons C16 and C17 at Site 1172.

3.2. Diatom Events

[16] Well-preserved, abundant and diverse marine diatom assemblages are recovered in the Eocene, across the E/O interval and throughout the Oligocene intervals at Sites 1170, 1171 and 1172. A continuous record of diatoms from the lowest middle Eocene up through the E/O interval was recovered at Site 1172 (base of Core 189-1172A-54X to -38X; ~503–350 mbsf; *Shipboard Scientific Party*, 2001a). A similar diatom assemblage from the lowest upper Eocene sediments across the E/O interval was also recovered at Sites 1170 and 1171 [*Shipboard Scientific Party*, 2001a, 2001c, 2001d; *Sluijs et al.*, 2003]. Absolute abundances are typically $\sim 2 \times 10^6$ to $\sim 40 \times 10^6$ valves/g sediment across the E/O transition interval in Hole 1172A (see also C. E. Stickley, manuscript in preparation, 2004). Eocene neritic diatoms are considered in situ on account of their high abundance, excellent preservation and association with typically shallow water dinocyst assemblages. Pyritized specimens also occur in lower abundance downcore from these horizons in Sites 1170–1172 and extend as far back as the latest Maastrichtian (Site 1172; *Schellenberg et al.* [2004]). In contrast, the Eocene interval of Site 1168 is barren of diatoms probably because a different water mass operated in the AAG at this time; see *Huber et al.* [2004] for full discussion of water mass characteristics.

[17] Three key Last Occurrence (LO) diatom events are recognized through the E/O transition interval of Hole 1172A (Figures 2a and 2b); *Distephanosira architecturalis* (~33.5 Ma; 358.8 mbsf), *Hemiaulus caracteristicus* (~33.5 Ma; 358.8 mbsf) and *Rocella vigilans* var. A sensu *Harwood and Maruyama* [1992] (~29 Ma; 353.6 mbsf). As noted by *Harwood and Maruyama* [1992], *R. vigilans* var. A is smaller and stratigraphically older than the larger (and younger) *R. vigilans* var. B sensu *Harwood and Maruyama* [1992]. In addition, the first occurrence (FO) datums of *Cavitatus jouseanus* (30.6 Ma) and *R. vigilans* var. A (30.2 Ma) co-occur at 357.39 mbsf (Figures 2a and 2b).

[18] The LO of *Hemiaulus caracteristicus* is generally widely reported in E/O sediments around the circum-Antarctic region making this event a potentially useful datum to mark the lowest Oligocene. It has not, so far, been robustly correlated to magnetostratigraphy for independent age control. However, it occurs near the base of Chron C13n in ODP Holes 744B and 748B (southern Kerguelen Plateau) [*Roberts et al.*, 2003] despite its rarity at these sites. Our broad re-interpretation of the diatom and paleomagnetic data reported in the Initial Reports of ODP 181, Site 1123 (N. Chatham Rise, SW Pacific) [*Shipboard Scientific Party*, 1999] also support this correlation. This datum is also observed in ODP Hole 1166A (Prydz Bay) by *Florindo et al.* [2003], who assign it a minimum age of ~33 Ma.

[19] The LO of *Distephanosira architecturalis* probably occurs slightly lower within Chron C13n than the LO of *Hemiaulus caracteristicus*. *Gombos and Ciesielski* [1983] and *Fenner* [1984] indicate a close succession of these two events at DSDP Site 511 (Falkland Plateau). In their studies, rare and stratigraphically sporadic occurrences above the last common occurrences of both these datums were regarded as reworked. Although the zonation of *Fenner* [1984] was not correlated to magnetostratigraphy, both datums are indicated to range above the LO of planktonic nannofossil *Reticulofenestra oamaruensis* at 33.7 Ma [*Berggren et al.*, 1995]. In ODP Hole 748B, *D. architecturalis* is more common than *H. caracteristicus* [*Harwood and Maruyama*, 1992], but their LO datums are coincident near the base of Chron C13n [*Roberts et al.*, 2003]. In Hole 1166A (Prydz Bay) the LO of *D. architecturalis* is assigned a minimum age of ~33 Ma [*Florindo et al.*, 2003].

[20] In Hole 1172A, both the LO of *D. architecturalis* and the LO of *H. caracteristicus* are associated with Chron C13n. Both of these events occur between samples at 359.06 mbsf and 358.71 mbsf, but we take both datums to occur at the same horizon (due to sequence condensation) at a depth of ~358.8 mbsf (Figures 2a and 2b) based on the position of a short paleomagnetic normal within this sampling range. This paleomagnetic normal is assigned to Chron C13n (see also *Fuller and Touchard* [2004], *Sluijs et al.* [2003], and *Stickley et al.* [2004]). A major hiatus is inferred at this horizon (358.8 mbsf), by the loss of dinocysts (see below). This hiatus marks the initiation of an interval of episodic scouring and winnowing that lasted until ~30.2 Ma, and resulted in the complete erosion/nondeposition of sediments representing Chron C12n and partly Chrons C12r and C11r (Figures 2a and 2b) (see below). Sporadic and very rare occurrences of *D. architecturalis* and *H. caracteristicus* within sediments representing Chron C12r are inferred as reworked.

[21] The FO datums of *Cavitatus jouseanus* and *Rocella vigilans* var. A co-occur between samples at 357.71 mbsf and 357.21 mbsf, which we take as 357.39 mbsf, corresponding to the base of the transitional chalk unit above the greensand (see materials and methods), ~9 cm below the base of Subchron C11n.2n (Figures 2a and 2b). Accordingly, they occur at the initiation of carbonate deposition, and the very end of presumed episodic erosion (see below). The lowermost range of *C. jouseanus* in Hole 1172A is probably therefore truncated since (1) this event is

reported to occur within Chron C12n in the Southern Ocean [*Baldauf and Barron*, 1991; *Harwood and Maruyama*, 1992; *Harwood et al.*, 1992; *Ramsay and Baldauf*, 1999; *Harwood and Bohaty*, 2001; *Roberts et al.*, 2003], and (2) its appearance at the base of the carbonates in Hole 1172A is very striking (i.e., a sudden abundance). In the Southern Ocean, the FO of *R. vigilans* var. A is reported to occur within Chron C11r [*Harwood and Maruyama*, 1992; *Gersonde et al.*, 1998; *Ramsay and Baldauf*, 1999], or near the base of Chron C11n.2n [*Roberts et al.*, 2003]; its lowermost range is, therefore, probably not significantly truncated at Site 1172. Thus essentially the entire *Cavitatus jouseanus* Partial Range Zone of *Harwood* [1986] (redefined by *Harwood and Maruyama* [1992]) is missing at Site 1172. *Fenner* [1984] notes problems in determining the exact position of the FO of *C. jouseanus* due to its rare and sporadic occurrence in the lowest part of its range. For this reason, *Harwood and Bohaty* [2001] suggest a conservative, slightly older occurrence for this datum within the upper part of Chron C12r, for the Southern Ocean. If this calibration is also applicable for the East Tasman Plateau, then the consistently high abundance of *C. jouseanus* throughout its lower range at Site 1172, testifies to the erosion of sediments below its FO at this site. Apparently, *C. jouseanus* first becomes consistently stratigraphically abundant near the FO of *R. vigilans* var. A at all Leg 189 sites. This First Abundant Occurrence datum may be a more useful event in the Southern Ocean than the FO suggested by *Harwood and Bohaty* [2001]. There is some variation in the morphology of *C. jouseanus* in the lowermost Oligocene of Hole 1172A, and we suggest that both *C. jouseanus* s.s. and *C. jouseanus* "early form" (sensu *Harwood and Bohaty* [2001] equals possibly *C. miocenicus* [*Barron*, 2004]), are present at the South Tasman Rise (C. E. Stickley, manuscript in preparation, 2004; Figure 2a). However, for the age model discussions presented in this paper, it has not been necessary to separate these two morphologies.

[22] The stratigraphic position of the FOs of *C. jouseanus* and *R. vigilans* var. A in Hole 1172A indicate that ~1.1 m of sediment representing Chron C12r lies unconformably beneath sediments of Chron 11r age (Figures 2a and 2b). Furthermore, the FO of *Rocella praenitida*, dated to 30.3 Ma by *Gersonde et al.* [1998], coincides with the FOs of *C. jouseanus* and *R. vigilans* var. A, verifying the presence of a thin interval (~9 cm) representing Chron C11r above 357.39 mbsf. However, we can not be precise about how much of C12r and C11r is missing, particularly since this combined long reversal represents an interval of episodic erosion and associated reworking (see below). *R. vigilans* vars A and B are separated stratigraphically by a distinct gap in ODP 189 sites (*Stickley et al.* [2004]; Figure 2a), as reported from the Kerguelen Plateau [*Harwood and Maruyama*, 1992; *Roberts et al.*, 2003]. The LO of *R. vigilans* var. A occurs near the top of Chron C10r (~29 Ma) on the Kerguelen Plateau [*Harwood and Maruyama*, 1992; *Roberts et al.*, 2003], and the East Tasman Plateau (this paper). Magnetostratigraphy at Site 1172 would suggest a long hiatus above this datum lasting until the late early Miocene [*Stickley et al.*, 2004], however, an abundance of *R. vigilans* var. B (range ~28–25 Ma) in a short interval at ~350.2 mbsf (*Stickley et al.* [2004] Figure 2a), suggests the presence of at least some sediment of late Oligocene age at Site 1172.

[23] The circum-Antarctic zonal marker *Rhizosolenia oligocaenica* could not be used at Site 1172 as almost all of its stratigraphic range (33.8–30.9 Ma; Chrons C13r to C12n) (*Harwood and Maruyama* [1992], recalibrated here to the *Berggren et al.* [1995] timescale; *Roberts et al.* [2003]) occurs in the early Oligocene hiatus/condensed section (see below). Almost the entire *R. oligoceanica* partial range zone of *Harwood et al.* [1989] (redefined by *Harwood and Maruyama*, 1992]) is missing. This species is known to have been present near Site 1172, however, as reworked specimens are observed in lower Oligocene sediments.

3.3. Organic-Walled Dinoflagellate Cyst (Dinocyst) Events

[24] The siliciclastic sediments (local subunit IIIA) are characterized by abundant marine and terrestrial palynomorphs. Dinocysts occur in high concentrations of ~15,000 dinocysts/g sediment on average [*Sluijs et al.*, 2003]. The overlying glauconitic unit (local unit II) contains increasingly less (~4000/g) dinocysts and terrestrial palynomorphs, which differ significantly in assemblage composition to those in local subunit IIIA beneath [*Sluijs et al.*, 2003]. Important qualitative and quantitative dinocyst events in the relevant interval at Site 1172 are discussed in detail by *Sluijs et al.* [2003] and *Brinkhuis et al.* [2003b], but a summary is provided below.

[25] Although the Paleocene-early Eocene dinocyst associations at Site 1172 already largely comprise typical Southern Hemisphere, or "endemic" taxa, endemism increased further still toward the end of the early Eocene [*Brinkhuis et al.*, 2003b]. The early/middle Eocene transition is marked by a strong influx of these Antarctic-endemic (or "transantarctic"; cf. *Wrenn and Beckmann* [1982]) species like *Arachnodinium antarcticum, Deflandrea antarctica, Enneadocysta* spp., *Octodinium askiniae* and *Vozzhennikovia* spp., and/or bipolar (high latitude) taxa like *Spinidinium macmurdoense* and the *Phthanoperidinium echinatum* group (see also, e.g., *Firth* [1996] and *Levy and Harwood* [2000]). This trend continued during the early late Eocene; "transantarctic" dinocysts predominate, and final acmes of *Enneadocysta* spp., the *Deflandrea antarctica* group and *Spinidinium macmurdoense* are recorded near the top of local subunit IIIA. Important FOs include those of *Aireiana verrucosa, Hemiplacophora semilunifera*, *Schematophora speciosa,* and *Stoveracysta ornata*. Also toward the top of local subunit IIIA, FOs of *Achomosphaera alcicornu*, *Reticulatosphaera actinocoronata* and notably *Alterbidinium distinctum* are important for interregional correlation. In addition, the LO of *Schematophora speciosa* (Figure 2b) is equally important, while *Phthanoperidinium* spp. and *Vozzhennikovia* spp. continue to be common. The LO of *Schematophora speciosa* is stratigraphically close to the slightly younger FO of *Stoveracysta kakanuiensis* in Hole 1172A (Figure 2b). A significant change in dinocyst associations, including a brief palynologically barren interval at Site 1172, occurs between these events (Figures 3 and 4). At the onset of the

glauconitic interval (360.6 mbsf), cosmopolitan taxa like *Cleistosphaeridium* spp., *Lingulodinium machaerophorum*, *Spiniferites* spp. and *Turbiosphaera filosa* become prominent, and undescribed species like *Brigantedinium*? sp. and *Deflandrea* sp. A begin to dominate. Slightly higher, in the succession near the E/O boundary (sensu the ''global stratotype section and point,'' GSSP, definition at Massignano, central Italy), sediments become conspicuously barren of organic microfossils. Only one sample from the lower Oligocene (Chron C11) (Figures 3 and 4) yielded dinocysts and in this sample (1172A-39X-2, 3–5 cm; 356.13 mbsf) virtually all ''transantarctic'' Paleogene dinocysts are absent (only a single, poorly preserved, probably reworked, specimen of *Enneadocysta partridgei* was recovered). The dinocyst association in this sample contains an abundance of taxa more typical for Tethyan waters, including an occurrence of *Hystrichokolpoma* sp. cf. *H. oceanicum* (compare, e.g., *Brinkhuis and Biffi* [1993], *Wilpshaar et al.* [1996], and *Brinkhuis et al.* [2003a]).

[26] Some of these late Eocene dinocyst events recorded at Site 1172, have been reported previously from the Browns Creek section (Victoria, Australia; see, e.g., *Cookson and Eisenack* [1965]). The ranges of several taxa appear useful for regional and even global correlation (e.g., *Aireiana verrucosa, Hemiplacophora semilunifera*, *Schematophora speciosa* and *Stoveracysta ornata*). Many of the late Eocene ''Browns Creek'' dinocysts have been recorded subsequently from locations around the world, most notably in central and northern Italy, including the Priabonian type section [*Brinkhuis and Biffi*, 1993; *Brinkhuis*, 1994]. It appears that these index species have slightly older LOs in the Tasmanian region than in the Tethyan region, if the records of *Cookson and Eisenack* [1965] and *Stover* [1975] are combined with more recent nannoplankton and magnetostratigraphic studies from the same section [*Shafik and Idnurm*, 1997]. These differences may be related to progressive cooling during the late Eocene, resulting in equatorward migration of subtropical and tropical species. Indications are that the LO of *S. speciosa* occurs within Chron C16 in the Tasmanian region (*Sluijs et al.* [2003]; Figure 2b). Information from Site 1168 [*Sluijs et al.*, 2003], Site 1172 [*Sluijs et al.*, 2003; this paper], Browns Creek and New Zealand sections (G. J. Wilson, personal communication, 2000), suggests the FO of *S. kakanuiensis* is associated with Chron C13r (Figure 2b). Importantly, this is the first dinocyst event that can be traced throughout the region, i.e., linking the AAG with the Pacific [*Sluijs et al.*, 2003]. The above events can be correlated confidently with associated palaeomagnetic and diatom information to other Leg 189 sites [see *Sluijs et al.*, 2003]. The more significant of these events are indicated in Figure 2b.

3.4. Isotope Stratigraphy

[27] Previous studies of planktonic and benthic foraminiferal $\delta^{18}O$ values established a globally recognized and marked step increase of ~0.8–1.2‰ across the E/O transition interval near the base of Chron 13n (e.g., DSDP Site 522 planktonic record of *Oberhänsli et al.* [1984]; global composite benthic record of *Zachos et al.* [2001]). This $\delta^{18}O$ step increase is known as the Oi-1 event [*Miller et al.*, 1991], and is attributed to major Antarctic cryosphere expansion and minor ocean cooling [*Lear et al.*, 2000; *Zachos et al.*, 2001]. *Bohaty and Zachos* [2003] report parallel $\delta^{18}O$ step increases of ~1‰ in both benthic foraminiferal and bulk (fine fraction) carbonate records through the E/O transition. Thus stratigraphic variations in bulk carbonate stable isotope values can provide a useful global correlation tool, although ecological shifts in carbonate contributors (i.e., nannoplankton and foraminiferal taxa with differing vital effects) and secondary diagenetic effects (i.e., incongruent dissolution, pore water/respiration-influenced precipitation) must also be considered [e.g., *Shackleton et al.*, 1993; *Bains et al.*, 1999].

[28] Bulk carbonate stable isotope analyses through the E/O transition interval in Hole 1172A reveal three distinct intervals that essentially coincide with (1) the siliciclastic carbonate-poor claystone of local subunit IIIA (>361.12 mbsf), (2) the ''carbonate-free'' glauconitic siltstone in the lower part of local unit II (361.12–357.39 mbsf), and (3) the carbonate-rich chalk (ooze) in the upper part of unit II to local subunit IC (<357.39 mbsf) (Figure 4). Average bulk carbonate $\delta^{18}O$ values are highly consistent within both the siliciclastic carbonate-poor claystone (-0.2 ± 0.1‰; n = 27) and carbonate-rich ooze (1.3 ± 0.2‰; n = 27), whereas $\delta^{18}O$ and $\delta^{13}C$ values within the ''carbonate-free'' glauconitic siltstone are highly variable and generally quite negative. We interpret the step increase of ~1.5‰ from the siliciclastic carbonate-poor claystone to the carbonate-rich ooze as evidence that the Oi-1 shift occurs somewhere within the ''carbonate-free'' glauconitic siltstone, where bulk carbonate $\delta^{18}O$ and $\delta^{13}C$ values from this essentially carbonate-free interval largely reflect isotopically negative diagenetic carbonate and remnant organic carbon. Thus, while these bulk carbonate isotopic data do not resolve the exact position of the Oi-1 event, they are independently consistent with biostratigraphic and magnetostratigraphic datums that position the Oi-1 event (i.e., base of Chron 13n) within the glauconitic siltstone. The inferred Oi-1 step increase of ~1.5‰ in Hole 1172A is somewhat greater than the typically observed ~0.8–1.2‰, and may reflect vital effects from carbonate contributors, regional evaporation-precipitation effects, and other mechanisms.

3.5. Integrated Results

[29] On the basis of the above biomagnetostratigraphic and stable isotopic data, we conclude that Cores -41X through -38X of Hole 1172A represent the late middle Eocene (Chron C17r) to the late early Oligocene (Chron C10r), with the E/O transition interval present in sections 3 and 4 of Core 39X (~358–360 mbsf). Diatom and dinocyst events (and middle-late Eocene cyclostratigraphy from *Röhl et al.* [2004]) help constrain the magnetochron assignments. The resulting age model is presented in Figures 2a and 2b. Our biomagnetostratigraphic age model highlights a series of erosional and/or nondeposition events that correlate with pronounced grain-size changes (Figure 4) and some taphonomic changes in diatoms and dinocysts (Figures 3 and 4). In addition, paleoceanographic events (discussed below)

indicated by diatom and dinocyst assemblage changes (Figures 3 and 4) can now be placed within a robust chronostratigraphic framework. Our Site 1172 age model can be correlated to Sites 1168, 1170 and 1171 based on results presented in the Leg 189 Scientific Results volume [see *Sluijs et al.*, 2003, Figure 2; *Brinkhuis et al.*, 2003a, 2003b; *Stickley et al.*, 2004], and indicate that the lithological changes recorded at Site 1172 are quasi-synchronous throughout the Tasmanian region. Locally, sedimentological character and sediment accumulation rates may differ, but a similar architecture and timing is apparent.

4. Nature of the Deepening of the Tasmanian Gateway

[30] The marine sequences recovered at Sites 1170 and 1171, located centrally within the Tasmanian Gateway demonstrate that the gateway was open to marine waters since at least the early Eocene [e.g., *Exon et al.*, 2001]. The Eocene successions at all Leg 189 sites are very shallow marine in nature [*Exon et al.*, 2001], and the subsequent onset of greensand deposition followed by carbonate deposition across all Leg 189 sites therefore heralds a major regional deepening of the Tasmanian Gateway [*Exon et al.*, 2001]. Paleomagnetic data indicate the onset of the greensand to have occurred at ~35.5 Ma, whereas diatom datums indicate the base of the carbonates has an age of ~30.2 Ma (Figures 2a and 2b). Moreover, other Leg 189 studies have shown that these lithological changes occurred synchronously throughout the region [e.g., *Sluijs et al.*, 2003].

[31] Considering (1) the completeness of the E/O transition interval at Site 1172, and (2) the high degree of biotic and lithostratigraphic similarity across Sites 1170, 1171, and 1172 in the Eocene, we consider Site 1172 to be representative of the central and eastern Tasmanian region. Our quantitative data from Site 1172 (Figures 3 and 4) strongly covary with the marked lithological changes, allowing recognition of four distinct phases in the environmental evolution of the Tasmanian Gateway: (A) Prior to ~35.5 Ma, (B) ~35.5–33.5 Ma, (C) ~33.5–30.2 Ma, and (D) after ~30.2 Ma.

4.1. Phase A: Middle to Early Late Eocene Pre-Gateway Deepening (Prior to ~35.5 Ma)

[32] During the middle to early late Eocene, the environment was characterized by an abundance of "endemic"-Antarctic, nearshore-neritic, planktonic and benthic diatom assemblages and endemic shallow-water dinocyst assemblages (Figures 3 and 4) preserved in claystones with relatively high linear sedimentation rates (i.e., ~2.6 cm/kyr average at the base of Chron C17r; Figure 2a). The relatively high wt % TOC and low wt % $CaCO_3$ values (Figure 4) are consistent with a prodeltaic marginal marine setting, while invariant bulk carbonate $\delta^{18}O$ and $\delta^{13}C$ values (Figure 4) are consistent with relatively stable environmental conditions. *Röhl et al.* [2004] record orbitally forced (Milankovitch) cyclical environmental changes during the Eocene (from at least 40 to 36 Ma) at Site 1172. These results reveal that an initial (minor) deepening had already occurred during Chron C17n times (line A1, Figures 3 and 4), prior to the first major deepening step (at ~35.5 Ma) outlined below.

[33] Middle to early late Eocene diatom assemblages at Site 1172 are characterized by abundant robust, shallow-water planktonic- and benthic-neritic marine taxa (Figure 3) similar to those reported by *Hajós* [1976] for DSDP Leg 29 sediments drilled on the South Tasman Rise. Some of these taxa may be endemic to the region to the south and east of Tasmania (Sites 1170, 1171 and 1172) and to the Ross Sea region, although offshore (oceanic) cosmopolitan diatoms are also occasionally present (Figures 3 and 4). Preservation is generally excellent with no discernable signs of dissolution and long colonial chains of benthic diatom frustules (e.g., *Paralia*) often intact, indicating an in situ flora within relatively quiet waters at depths of <50 m. Colonial chains become notably less intact following the first deepening step at ~35.5 Ma, which may reflect strengthening bottom currents although postdepositional fragmentation cannot be excluded. The most abundant diatom taxa are species of the robust, relatively large, planktonic genera *Hemiaulus*, *Pyxilla* and *Stephanopyxis*, along with species of the benthic and/or tychopelagic (benthics dislodged into plankton) genera *Actinoptychus*, *Arachnoidiscus*, *Biddulphia* (and related taxa), *Distephanosira*, *Hyalodiscus*, *Melosira*, *Paralia*, *Podosira/Pseudopodosira*. Relative abundance data are from a total minus *Pyxilla* spp., *Stephanopyxis grunowii* and *S. turris* in order to emphasize trends in less predominant taxa. A generally high species richness and a large proportion of resting spores (e.g., of the genera *Chaetoceros* group, *Goniothecium*, *Pterotheca* and *Xanthiopyxis*; Figure 3) indicate eutrophic conditions likely stimulated by periodic terrestrial runoff. This interpretation is supported by a generally good agreement in abundance changes between terrestrial palynomorphs, chrysophyte cysts (data not shown) and eutrophic diatom and dinocyst indicators. *Chaetoceros* resting spores appear to be more abundant just prior to the first major deepening step at ~35.5 Ma (Figure 3), perhaps indicating increased terrestrial runoff at this time.

[34] A literature review of diatoms reported from middle Eocene and E/O sediments globally has allowed us to identify a possible Eocene Antarctic "endemic" diatom flora. The biogeography of the flora matches a proposed clockwise-rotating regional "proto-Ross Sea Gyre" (Figure 5; *Huber et al.* [2004]) rather than a southbound subtropical East Australian Current sensu [*Murphy and Kennett*, 1986]. We emphasize that this "endemic" flora is distinct and separate from the Neogene and younger endemic Antarctic flora associated with a well-developed ACC. While the total biogeographic extent of this Antarctic Eocene endemic flora remains uncertain, there seems to be an affinity of the floras recovered in the Tasmanian Gateway (e.g., those reported by *Hajós* [1976]; this paper; C. E. Stickley, manuscript in preparation, 2004] with those reported from the McMurdo Sound and Ross Sea region, from at least the middle Eocene until possibly ~32 Ma (at Site 1172; see also *Huber et al.* [2004]). For example, although the information on middle Eocene diatoms is sparse in both high and lower latitudes, many of the taxa reported from the Ross Sea area of roughly equivalent age

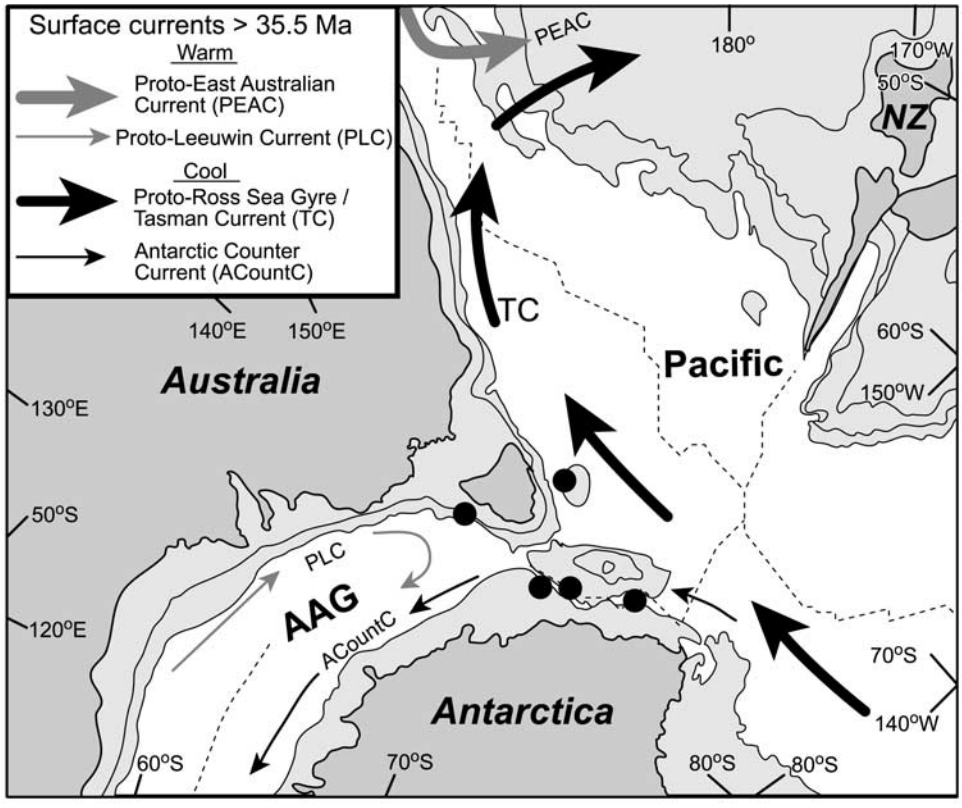

Figure 5. Reconstruction of inferred surface water circulation in the Tasmanian Gateway, prior to gateway deepening, during late evolutionary phase A (>35.5 Ma; late Eocene). The reconstruction is based on field data (this paper) and modeling results [*Huber et al.*, 2004]. Black circles, ODP Leg 189 drill sites; dotted lines, plate tectonic reconstruction; AAG, Australo-Antarctic Gulf; NZ, New Zealand. Warm currents: PEAC, Proto-East Australian Current; PLC, Proto-Leeuwin Current. Cool currents: Proto-Ross Sea Gyre, of which the Tasman Current, TC [*Huber et al.*, 2004], is a limb, and an "Antarctic Counter Current" (ACountC). Relative current strength is implied by arrow size. Note the direction and strong influence of the cool TC on the Antarctic and East Australian margins. The ACountC is indicated by both field [*Brinkhuis et al.*, 2003a] and modeling data [*Huber et al.*, 2004]. Modified from *Shipboard Scientific Party* [2001e].

[e.g., *Harwood*, 1989; *Harwood and Bohaty*, 2000] are also present at Site 1172 (see diatom analysis for a list of taxa). In addition, many undescribed taxa recovered in the Eocene of Sites 1170, 1171 and 1172 are assumed to be endemic (formal descriptions of these taxa are underway). Not unexpectedly, Eocene floras from Sites 1170–1172 bear little resemblance to those reported from age-equivalent tropical-subtropical sediments [e.g., *Holmes and Brigger*, 1977; *Fenner*, 1984; *Fenner and Mikkelsen*, 1990; *Baldauf*, 1992], given that many typical Tethyan warm-water Eocene taxa are absent. Furthermore, in contrast to the implications by *Hajós* [1976], we consider the upper Eocene diatom floras at Sites 1170–1172 to bear only a minimal resemblance to the coeval flora of the Oamaru Diatomite [e.g., *Desikachary and Sreelatha*, 1989; *Edwards*, 1991] of New Zealand, which appears to have been under the influence of warmer waters, than Sites 1170–1172, at that time [*Huber et al.*, 2004]. Some of the diatoms we assign to our endemic category may be restricted only in the middle Eocene, becoming more widespread within the greater circum-Antarctic region through the latest Eocene/earliest Oligocene, e.g., *H. caracteristicus*, present in the middle Eocene of the East Tasman Plateau (Hole 1172A), is not reported from coeval sediments on the Falkland Plateau (DSDP Hole 512; see *Gombos* [1983]), but appears there in upper Eocene sediments (DSDP Hole 511; see *Gombos and Ciesielski* [1983]). Additionally, some of the middle Eocene diatoms reported from the Falkland Plateau by, e.g., *Gombos* [1983] (i.e., *Bergonia angelica*, species of *Rylandsia* and *Tubaformis unicornis*) are not present at ODP 189 sites. Our findings corroborate those of *Harwood* [1991] who noted some biogeographical differences between the lower Oligocene diatom assemblages from the Ross Sea region (e.g., CIROS-1 drillhole), with those from both East Antarctica and the Southern Ocean (e.g., Falkland Plateau), prior to the development of significant deep-water flow through the Tasmanian Gateway.

[35] Periodic increases in more offshore diatoms (e.g., *Actinocyclus*, *Azpeitia*, *Cestodiscus*, *Coscinodiscus*, *Rhizosolenia*, *Rouxia* and *Trinacria/Triceratium/*

Sheshukovia informal group) through the middle and upper Eocene (Figures 3 and 4) sediments of Hole 1172A may be related to small-scale sea level variations inferred by *Röhl et al.* [2004]. Similar pulses have been recognized in coeval sediments at Sites 1170 and 1171 (CES unpublished data). These offshore taxa are characterized by cosmopolitan species *Coscinodiscus marginatus*, *C. radiatus* and the middle Eocene marker *Triceratium inconspicuum* var. *trilobata*.

[36] A dinocyst association of the *Deflandrea antarctica* group, *Enneadocysta* spp., *Phthanoperidinium* spp., *Spinidinium* spp., and *Vozzhennikovia* spp. occurs throughout middle to lower upper Eocene sediments at Sites 1170–1172 [see also *Shipboard Scientific Party*, 2001a, 2001c, 2001d; *Brinkhuis et al.*, 2003b; *Sluijs et al.*, 2003], but is absent from coeval sediments at Site 1168 [*Brinkhuis et al.*, 2003a; *Sluijs et al.*, 2003]. Peridinioid cysts (Figure 3) such as *Deflandrea* spp., *Phthanoperidinium* spp., *Spinidinium* spp. and *Vozzhennikovia* spp. commonly dominate this association. Extensive empirical evidence [see *Brinkhuis et al.*, 1992; *Brinkhuis*, 1994; *Firth*, 1996; *Stover et al.*, 1996] suggest that these cysts represent marginal marine heterotrophic dinoflagellates that are closely tied to deltaic settings, diatom abundances, and organic-rich facies.

[37] Besides the Tasman region [e.g., *Haskell and Wilson*, 1975; *Kemp*, 1975; *Crouch and Hollis*, 1996; *Truswell*, 1997], this Antarctic endemic association of dinoflagellates (Figures 3 and 4) has also been found in the Eocene of McMurdo Sound [e.g., *Wilson*, 1967; *Hannah and Raine*, 1997; *Levy and Harwood*, 2000], the Ross Sea [*Wrenn et al.*, 1998], Seymour Island/Weddell Sea [*Wrenn and Hart*, 1988; *Mohr*, 1990], Bruce Bank/Scotia Sea [*Mao and Mohr*, 1995], Falkland Plateau [*Goodman and Ford*, 1983], Prydz Bay/Mac.Robertson Shelf [*Quilty et al.*, 1999], and Argentina [*Guerstein et al.*, 2002, and references therein], and is thus widespread throughout the Antarctic region to paleolatitudes of about 60° South. As for the co-occurring diatom floras, the biogeography of this highly Antarctic-endemic dinocyst association matches the proposed clockwise-rotating regional "proto-Ross Sea Gyre" (Figure 5; *Huber et al.* [2004]). However, typical cosmopolitan dinocysts like *Spiniferites* spp., *Thalassiphora pelagica* co-occur with the endemic taxa to a certain extent.

4.2. Phase B: Deepening and Inception of Energetic Bottom Currents (35.5–33.5 Ma)

[38] At ~35.5 Ma (line B1; ~360.3 mbsf; Figures 3 and 4), subsidence acceleration and basin deepening are inferred by the abrupt appearance and rapid development of new diatom and dinocyst assemblages dominated by offshore taxa indicative of high-nutrient offshore settings (e.g., upwelling) rather than prodeltaic settings (Figures 3 and 4). At the same time, the inception of more energetic bottom currents is inferred from a notable increase in grain size (Figure 4) and inception of authigenic glauconites, suggesting an increase in winnowing. This switch in dominance from shallow- to deeper-water diatom taxa immediately follows a notable but brief increase in shallow-water neritic diatoms (~361–360.0 mbsf; Figure 3), high nutrient diatom indicators and sedimentation rates. This transient change indicates that just prior to the inception of bottom-water activity there was a brief period of increased runoff, decelerated subsidence rates, or interplay of both (line A2, Figures 3 and 4).

[39] Endemic and neritic diatom taxa (e.g., *Actinoptychus*, *Arachnodiscus*, *Biddulphia*, *Hyalodiscus*, *Paralia Podosira* and *Pterotheca*) decrease significantly between ~35.5 and 33.5 Ma (lines B1 to C1, Figure 3). This group is progressively exceeded in abundance up core by cosmopolitan and offshore (oceanic) taxa (Figures 3 and 4) such as species of *Actinocyclus*, *Asteromphalus*, *Azpeitia*, *Coscinodiscus*, *Cestodiscus* and *Rhizosolenia*. Some of these oceanic taxa were already present at background levels throughout the Eocene; others appear for the first time.

[40] Coeval grain-size data highlight associated increases in winnowing (i.e., hiatuses and/or condensation), notably at the onset of and through Subchron C16n.1n (Figure 4), culminating in the coarsest grain size (~64.4 μm average) of this interval. Concomitant abundances of the relatively large dinocyst *Deflandrea*, and diatoms *Pyxilla* and *Stephanopyxis* may be related to this winnowing effect. We use the relative abundance of *Pyxilla* and *Stephanopyxis* along with general diatom preservation as a further indication of winnowing (Figure 2a). This interval of relatively large sediment particles occurring at ~360.3 mbsf (~35.5 Ma) corresponds to a notable increase in sediment sorting and a brief depositional hiatus, which probably represents the first discernable record of increased regional bottom-water currents. The hiatus lasted for ~300 kyr ending at ~35.2 Ma with the first abundant occurrence (FAO) of *Brigantedinium*? sp. (see below). Such energetic bottom-water currents may be associated with stronger (wind-driven) circulation through the Tasmanian Gateway, and into the Pacific, given that other evidence discussed above indicates deeper, offshore settings at this time relative to the initial middle Eocene shallow marine conditions. The hiatus most probably occurs at the base of a short palynologically barren interval and associated low wt % TOC (Figures 3 and 4), which also support increased winnowing and/or oxygenation. Furthermore, the onset of Subchron C16n.1n is marked by a decrease in wt % $CaCO_3$ from ~5% to ~0–1% (Figure 4). This decrease likely results from a combination of decreased carbonate export production, increased carbonate fine-fraction winnowing, and intensified carbonate dissolution. A few organic foraminiferal linings recorded in the palynological samples indicate the initial presence of benthic foraminifera and their subsequent test dissolution. Moreover, the inferred initiation of bottom-water currents coincides with an increase in glauconite within a highly condensed section as sedimentation rates fell to an average of <1 mm/kyr.

[41] Palynomorph preservation returns again in the middle of Chron C15r (~35.2 Ma; line B2; ~360.0 mbsf; Figures 3 and 4), and the prodeltaic dinocyst association is abruptly (but more gradually at Sites 1170–1171; see *Sluijs et al.* [2003]) replaced by associations dominated by *Brigantedinium*? sp. and *Deflandrea* sp. A. In modern oceans, *Brigantedinium* is characteristic of oceanic upwelling regions [e.g., *Dale*, 1996; *Rochon et al.*, 1999], representing hetererotrophic dinoflagellates in the

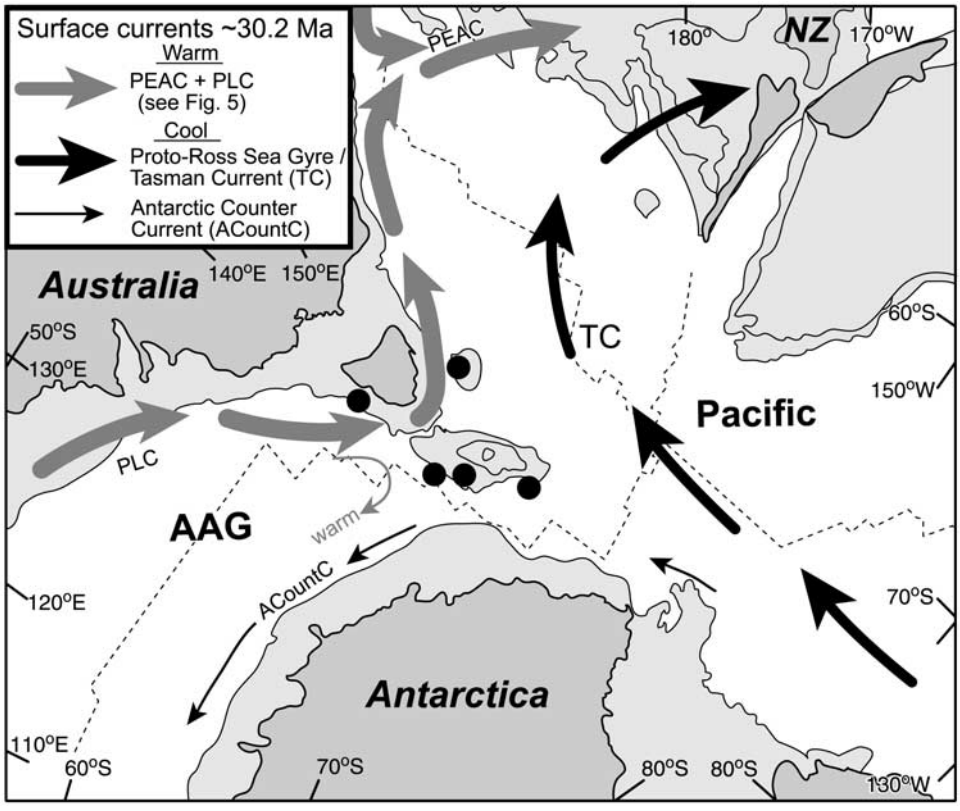

Figure 6. Reconstruction of inferred surface water circulation in the Tasmanian Gateway, post gateway deepening, during early evolutionary phase D (~30.2 Ma; early Oligocene). The reconstruction is based on field data (this paper) and modeling results [*Huber et al.*, 2004]. Black circles, ODP Leg 189 drill sites; dotted lines, plate tectonic reconstruction; AAG, Australo-Antarctic Gulf; NZ, New Zealand. Warm currents: PEAC, Proto-East Australian Current; PLC, Proto-Leeuwin Current. Cool currents: Proto-Ross Sea Gyre, of which the Tasman Current, TC [*Huber et al.*, 2004], is a limb, and an "Antarctic Counter Current" (ACountC). Relative current strength is implied by arrow size. Note the influence of warm, AAG-derived water on the gateway. The ACountC is indicated by both field [*Brinkhuis et al.*, 2003a] and modeling data [*Huber et al.*, 2004]. Modified from *Shipboard Scientific Party* [2001e].

Protoperidinium group, which typically feed on diatoms. The First Abundant Occurrence (FAO) of *Brigantedinium*? sp. (Figure 2b) indicates the inception of an oceanic upwelling system or cell on a rather large scale at ~35.2 Ma. At Sites 1170 and 1171 *Brigantedinium?* sp., and other Protoperidinioid (heterotrophic) taxa such as *Octodinium askiniae* and *Selenopemphix* spp. become abundant at ~35.2 Ma [*Sluijs et al.*, 2003]. Despite a significant offshore influence, shallow-water diatom and dinocyst taxa remain relatively abundant until ~33.5 Ma (Figure 3), suggesting still only relatively shallow to intermediate depths (outer neritic to upper bathyal).

[42] Combined dinocyst information from all Leg 189 sites shows that the FO of *Stoveracysta kakanuiensis* in the lower part of C13r (~359.5 mbsf in Hole 1172A; Figure 2b) is the oldest event that can be correlated throughout the entire region from South Australia to New Zealand [*Sluijs et al.*, 2003]. This species was first described from the "latest Eocene" of New Zealand [*Clowes*, 1985], and appears to mark the arrival of "new" surface water conditions influencing sites throughout the entire region from ~34.5 Ma onward (line B3; ~359.5 mbsf; Figures 3 and 4). As argued by *Huber et al.* [2004], these surface waters originated from an eastward flowing "proto-Leeuwin Current" from the AAG and/or the effect of the injection of such waters into the proto-Ross Sea Gyre heading toward Site 1172 (Figure 6; *Huber et al.* [2004]); i.e., relatively warmer surface waters originating in the Indian Ocean influenced the Tasmanian Gateway from ~34.5 Ma onward, rather than colder surface waters as the Tasmanian Gateway Hypothesis would suggest.

4.3. Phase C: Further Deepening and Intensification of Energetic Bottom Currents (33.5–30.2 Ma)

[43] Several lines of evidence support a second, more extensive, hiatus at ~33.5 Ma (line C1; 358.8 mbsf; Figures 3 and 4) marking intensified bottom-water activity, further deepening and increased oxygenation. Here, an increase in grain size is associated with the abrupt disappearance of all palynomorphs [see also *Brinkhuis et al.*, 2003a, 2003b], a decrease in wt % TOC, and an increase in abundance of oceanic diatoms (Figures 3 and 4).

Furthermore, at Sites 1170–1172 there is an increase in the previously rare "cosmopolitan" oceanic taxa derived from Subantarctic and temperate planktonic flora, a shift consistent with the inception of warm surface water sourcing throughout the Tasmanian Gateway region. Moreover, at this level the biostratigraphic marker taxa *Distephanosira architecturalis* and *Hemiaulus caracteristicus* disappear (see age model; Figures 2a and 2b). Scouring and winnowing occurred periodically until the onset of carbonate ooze deposition at ~30.2 Ma, as suggested by grain-size data, visual inspection of the sediments [*Shipboard Scientific Party*, 2001a], and the inferred absence of sediments representing Subchron C12n (see age model). These hiatuses may in part relate to the sea level changes associated with the onset of the Antarctic cryosphere and the Oi-1 event, but conclusive evidence is absent. A thin core interval (one sample) within the long paleomagnetic reversal assigned to Subchrons C12r-C11r, is completely barren of diatoms and contains a grain-size peak. This thin interval represents significant winnowing and/or erosion, and likely corresponds to the hiatus containing the missing Subchron C12n interval. Linear sedimentation rates [e.g., *Stickley et al.*, 2004] indicate the hiatus to have commenced at ~32 Ma (line C2; ~358.4 mbsf; Figures 3 and 4). Significantly, the last occurrence of endemic diatoms at Site 1172 occurs at this hiatus. Just prior to the hiatus, endemic diatoms comprise 60% of the assemblage (excluding predominant taxa, see Figure 3 caption) but fall to zero immediately afterward and remain absent thereafter (Figures 3 and 4). This assemblage change is consistent with the inferred inflow of warmer waters from the northern AAG or a "proto Leeuwin Current" into the southern Pacific Ross Sea gyre at this time [see *Huber et al.*, 2004].

[44] Reworked diatoms are common across the entire interval of scouring (33.5 to 30.2 Ma; lines C2 to D1, Figures 3 and 4). The absence of dinocysts and other organic matter in Oligocene sediments from 33.5 Ma onward suggests highly oxygenated waters, low sediment accumulation rates, and/or winnowing [see *Brinkhuis et al.*, 2003b]. The very low abundance of diatom nutrient indicators and the corresponding higher abundance of oceanic cosmopolitan (more oligotrophic) diatoms suggest oligotrophic open-ocean conditions (a brief perturbation in the trend between lines C2 and D1 are caused by a fall in total diatom abundance). However, after 35.5 Ma and again after 33.5 Ma, isolated peaks within the trend of decreasing neritic diatoms (Figure 3) may indicate episodic upwelling, and/or associated periodic seaward transport of shallow material. The latter may be taken to indicate that Site 1172 was still sufficiently close to land. Nevertheless, the paucity of diatom nutrient indicators after ~33.5 Ma suggests the nutrient supply was relatively limited and waters were predominantly oligotrophic.

4.4. Phase D: Postgateway Opening, Fully Offshore Pelagic Environments (<30.2 Ma)

[45] The coappearance of diatom markers *Cavitatus jouseanus* and *Rocella vigilans* var. A marks the return of deposition and inception of the "transitional chalk" interval (forming the upper part of local unit II) (line D1; 357.39 mbsf; Figures 3 and 4). This transitional interval is characterized by an increase to ~20 wt % $CaCO_3$ (Figure 4) and abundant calcareous nannofossils and planktonic foraminifera [*Shipboard Scientific Party*, 2001a]. Bulk carbonate $\delta^{18}O$ values are ~1.5‰ higher than those below the greensand in local subunit IIIA (Figure 4), confirming a post Oi-1 age [*Miller et al.*, 1991; *Zachos et al.*, 1996]. We have dated the base of the "transitional chalk" interval (357.39 mbsf) at ~30.2 Ma based on the FO of *R. vigilans* var. A (see age model). This "transitional chalk" coincides with a conspicuous reduction in mean grain size (Figure 4) and is interpreted as the end of the intense scouring/erosion that began at 35.5 Ma and intensified at 33.5 Ma. The "transitional chalk" also signals the onset of a fully offshore pelagic environment away from any terrestrial influences and represents the final (and perhaps the most abrupt) deepening phase of Tasmanian Gateway opening during the E/O transition. Importantly, no evidence for ice-rafting has been recorded. The top of the "transitional chalk" (base of local subunit IC) is marked by a sharp increase to ~50 wt % $CaCO_3$ at the base of Subchron C11n.1n (29.7 Ma; 355.8 mbsf; Figure 4). Increased sediment accumulation rates increased from the base of the "transitional chalk" (Figure 2a) are attributed mainly to increased calcareous microfossil production and export.

[46] The carbonate-rich intervals of the E/O transition (the "transitional chalk" interval of the upper part of local unit II, and the siliceous-rich carbonate ooze of local subunit IC) are characterized by abundant cosmopolitan open-ocean diatoms and continued floristic turnover (Figures 3 and 4). The increase in cosmopolitan open-ocean diatoms occurred in two steps: the first step at ~30.2 Ma occurred through the lower half of the "transitional chalk," while the second and more significant step (at the termination of subchron C11n.2n; 29.8 Ma) occurred through the upper half of the "transitional chalk" and into subunit IC (Figures 3 and 4). Significantly, the diatom assemblages consist almost entirely of cosmopolitan open-ocean diatoms within subunit IC. The second step is characterized by an acme in just a few species (mainly those that appeared during the first step (e.g., *C. jouseanus* "early form," *R. praenitida* and *R. vigilans* var. A)) plus the appearance of several new species but particularly *C. jouseanus* s.s (Figure 2a) and *Cestodiscus* spp.

[47] The dinocysts preserved in the upper part of the "transitional chalk" in only one Site 1172 sample (Figures 3 and 4), approximately correspond to the second step increase in cosmopolitan open-ocean diatoms. Conspicuously, this dinocyst assemblage is also composed of offshore, warm to warm-temperate taxa (e.g., *Hystrichokolpoma* spp., *Hystrichokolpoma* sp. cf. *H. oceanicum, Spiniferites* spp.). The preservation of such organic remains must indicate less rigorous ventilation and/or higher sedimentation rates, possibly in association with warmer surface waters. Moreover, the matching oceanic and cosmopolitan character of both microfossil assemblages supports warmer rather than colder water masses influencing Site 1172 at this time (Figure 6). In addition, the coappearance of cosmopolitan diatoms (*C. jouseanus*, *R. praenitida*, *R. vigilans* var. A) at the base of the "transitional chalk" at Sites 1170, 1171 [*Sluijs*

et al., 2003], and 1172 indicates that by 30.2 Ma the Tasmanian Gateway had deepened significantly to fully connect the former AAG and the southern Pacific via the eastward flow of water masses originating within the AAG or southeastern Indian Ocean. It may be argued that the apparent influence of relatively warm, oligotrophic waters during the early Oligocene at Site 1172 alone results from intensification, or increased proximity, of the East Australian Current (EAC) as proposed by e.g., *Murphy and Kennett* [1986]. However, this scenario would necessitate invoking a strengthening of the EAC precisely when *Murphy and Kennett* [1986] propose it should be weakening, and also require increased ocean heat transport in the early Oligocene, which is the opposite conclusion to that reached by *Murphy and Kennett* [1986]. In addition, as discussed in depth by *Huber et al.* [2004], the overall change in middle Eocene to early Oligocene biogeographic patterns at ODP Leg 189 sites and the broader region (cf. compilation of biogeographic data in the work of *Huber et al.* [2004]), together with results from fully coupled GCM experiments [*Huber et al.*, 2004], are difficult to reconcile with the concept advocated by *Murphy and Kennett* [1986] and *Exon et al.* [2001]. Rather than assuming an increased influence of the EAC solely at Site 1172 and a "proto-ACC" flowing through the Tasmanian Gateway to the south, we favor the scenario that Tasmanian Gateway deepening led to the inflow of relatively warm AAG waters into a northbound "Tasman Current" (Figure 6), part of the southern Pacific Proto-Ross Sea Gyre that had existed since Cretaceous times [*Huber et al.*, 2004]. This scenario is consistent with regional surface water warming around south and east Tasmania during the early Oligocene and the disappearance of endemic Antarctic biota in its flow path. In any event, our study lends no support for an early (E/O) inception of a "proto-ACC" current regime influencing the region until sometime after the middle Oligocene.

5. Conclusions

[48] Integration of quantitative sedimentological, geochemical, paleomagnetic and biostratigraphic data reveal stepwise environmental changes through the E/O transition interval at Site 1172, reflecting the deepening of the Tasmanian Gateway. The following events characterize the four evolutionary phases A–D (lines A1–D1; Figures 3 and 4):

5.1. Phase A: Prior to ~35.5 Ma

[49] Middle to early late Eocene, premajor gateway deepening, shallow marine, eutrophic, prodeltaic settings (see Figure 5), with the following characters: (A1) initial minor deepening during the onset of Chron C17n; (A2) brief return to moderate sedimentation rates during Subchron C16n.1n.

5.2. Phase B: ~35.5 to ~33.5 Ma

[50] Latest Eocene, the onset of glauconitic deposition, deepening of the Tasmanian Gateway, and a shift to more open-oceanic nutrient-rich setting, with (B1) inception of energetic bottom-water currents at ~35.5 Ma, inducing winnowing and relatively moderate seafloor erosion which lasted ~300 kyr (to ~35.2 Ma); (B2) larger-scale oceanic nutrient rich settings (upwelling) established by ~35.2 Ma; and (B3) first indication of surface water connection between the eastern and western areas of the Tasmanian Gateway at ~34.5 Ma.

5.3. Phase C: ~33.5 to ~30.2 Ma

[51] Earliest Oligocene, intensified deepening and episodic erosion by progressively more energetic bottom-water currents, arrival of oligotrophic oceanic settings, e.g., (C1) intensification of energetic bottom-water currents at ~33.5 Ma allowing further winnowing and erosion which lasted for ~3 Myr (to ~30.2 Ma) including notably; (C2) disappearance of endemic Antarctic phytoplankton; a hiatus at ~32 Ma, followed by the inception of oceanic, oligotrophic, warm-temperate conditions; no evidence for decreasing sea surface temperatures.

5.4. Phase D: After ~30.2 Ma

[52] Early Oligocene, fully offshore, pelagic, oligotrophic, warm-temperate conditions (Figure 6), characterized by: (D1) carbonate ooze (chalk) deposition with a consistent influx of cosmopolitan phytoplankton marking the end of the interval of episodic erosion.

[53] Our findings indicate that (1) the Tasmanian Gateway deepened at least 1.8 Myr (at ~35.5 Ma) before the E/O boundary, sensu GSSP (33.7 Ma), (2) the widely recognized earliest Oligocene cooling event associated with Chron C13n (Oi-1 event; *Miller et al.* [1991]; *Zachos et al.* [1996]) and the E/O transition itself (mid Chron C13r to the base Chron C12r) are represented by a condensed interval and/or series of hiatuses, which (3) represent the most significant increase in deepening and associated bottom-water current activity in the Tasmanian Gateway. (4) These records carry no apparent signal of sea-surface temperature decrease, but rather (5) that earliest Oligocene sea-surface temperatures increased, and that (6) a stable, deep-marine setting consistently influenced by relatively warm surface waters was established by the onset of Chron C11. Our findings of apparent sea-surface temperature warming during the earliest Oligocene support the findings of *Lear et al.* [2000].

[54] Our geological data are consistent with independent modeling results, which suggest that Tasmanian Gateway deepening led to the inflow of relatively warm AAG waters through the Tasmanian Gateway into the southern Pacific Proto-Ross Sea Gyre (Figures 5 and 6; *Huber et al.* [2004]) in turn leading to significant warming of surface waters in the area off south and east Tasmania during the early Oligocene, and the disappearance of endemic Antarctic biota in its path. Our study lends no support for (1) a decrease in the import of warm water into this high latitude region (i.e., no increase in Antarctic thermal isolation), and therefore (2) no early (E/O) inception of a "proto-ACC" current influencing the region.

[55] **Acknowledgments.** This research used samples and data provided by the Ocean Drilling Program (ODP). ODP is sponsored by the U.S. National Science Foundation (NSF) and participating countries under management of Joint Oceanographic Institutions (JOI) Incorporated. Funding for this research was provided by US and international agencies: the Natural Environment Research Council (NERC)/UK-ODP to CES, the Joint Oceanographic Institutes U.S. Science Support (JOI/USSSP) and National

Science Foundation (NSF) to SAS, and by the Deutsche Forschungsgemeinschaft (DFG) to U. Röhl. CES gratefully acknowledges the Environmental Change Research Centre (University College London, UK) and Lamont-Doherty Earth Observatory. MG thanks Morten Perjup, Institute of Geography, University of Copenhagen, Denmark, for instrumental access (grain size). We thank Natasja Welters and Jan van Tongeren (Utrecht) for palynological sample processing. HB, AS and JW gratefully acknowledges NWO, the Netherlands Organization for Scientific Research. Thanks to Neville Exon, David Harwood, James Kennett, James Powell and Patrick Quilty for their comments and suggestions for improvements to an earlier version of this manuscript. We thank John Barron and Jim Riding for their thorough reviews of the current manuscript and Larry Peterson for editorial comments. CES also thanks Steve Bohaty for helpful comments to the paper and discussions on Southern Ocean E/O diatom biostratigraphy, and to Martin Pearce for discussions and improvements to the text and figures.

References

Agrawal, Y. C., I. N. McCave, and J. B. Riley (1991), Laser diffraction size analysis, in *Principles, Methods, and Application of Particle Size Analysis*, edited by J. P. M. Syvitski, pp. 119–128, Cambridge Univ. Press, New York.

Bains, S., R. M. Corfield, and R. D. Norris (1999), Mechanisms of climate warming at the end of the Paleocene, *Science*, *285*, 724–727.

Baldauf, J. G. (1992), Middle Eocene through early Miocene diatom floral turnover, in *Eocene-Oligocene Climatic and Biotic Evolution*, edited by D. R. Prothero and W. A. Berggren, pp. 310–326, Princeton Univ. Press, Princeton, N. J.

Baldauf, J. G., and J. A. Barron (1991), Diatom biostratigraphy: Kerguelen Plateau and Prydz Bay regions of the Southern Ocean, *Proc. Ocean Drill. Program Sci. Results*, *119*, 547–598.

Barker, P. F. (2001), Scotia Sea regional tectonic evolution: Implications for mantle flow and palaeocirculation, *Earth Sci. Rev.*, *55*, 1–39.

Barron, J. A. (2004), Planktonic marine diatom events of the Oligocene and earliest Miocene in the Equatorial Pacific Ocean, in *Commemorative Volume in Honour of Professor M. S. Srinivasan*, edited by D. Sinha, Narosa Publ., New Dehli, India, in press.

Battarbee, R. W. (1986), Diatom analysis, in *Handbook of Holocene Palaeoecology and Palaeohydrology*, edited by B. E. Berglund, pp. 527–570, John Wiley, Hoboken, N. J.

Battarbee, R. W., and M. J. Kneen (1982), The use of electronically counted microspheres in absolute diatom analysis, *Limnol. Oceanogr.*, *27*, 184–188.

Berggren, W. A., D. V. Kent, C. C. Swisher III, and M.-P. Aubry (1995), A revised Cenozoic geochronology and chronostratigraphy, in *Geochronology, Time Scales and Global Stratigraphic Correlations: A Unified Temporal Framework for a Historical Geology*, *Spec. Publ. Spec.*, vol. 54, edited by W. A. Berggren, D. V. Kent, and J. Hardenbol, pp. 129–212, Soc. for Sediment. Geol., Tulsa, Okla.

Bohaty, S. M., and J. C. Zachos (2003), Significant Southern Ocean warming event in the late middle Eocene, *Geology*, *31*, 1017–1020.

Brinkhuis, H. (1994), Late Eocene to Early Oligocene dinoflagellate cysts from the Priabonian type-area (northeast Italy): Biostratigraphy and palaeoenvironmental interpretation, *Palaeogeogr. Palaeoclimatol. Palaeoecol.*, *107*, 121–163.

Brinkhuis, H., and U. Biffi (1993), Dinoflagellate cyst stratigraphy of the Eocene/Oligocene transition in central Italy, *Mar. Micropaleontol.*, *22*, 131–183.

Brinkhuis, H., A. J. Powell, and D. Zevenboom (1992), High-resolution dinoflagellate cyst stratigraphy of the Oligocene/Miocene transition interval in northwest and central Italy, in *Volume on Neogene and Quaternary Dinoflagellate Cysts and Acritarchs*, edited by M. J. Head and J. H. Wrenn, pp. 219–258, Am. Assoc. of Stratigr. Palynol. Found., Salt Lake City, Utah.

Brinkhuis, H., D. M. Munsterman, S. Sengers, A. Sluijs, J. Warnaar, and G. L. Williams (2003a), Late Eocene to Quaternary dinoflagellate cysts from ODP Site 1168, off western Tasmania, *Proc. Ocean Drill. Program Sci. Results*, *189*, 1–36. (Available at http://www-odp.tamu.edu/publications/189_SR/VOLUME/CHAPTERS/105.PDF)

Brinkhuis, H., S. Sengers, A. Sluijs, J. Warnaar, and G. L. Williams (2003b), Latest Cretaceous to earliest Oligocene, and Quaternary dinoflagellate cysts from ODP Site 1172, East Tasman Plateau, *Proc. Ocean Drill. Program Sci. Results*, *189*, 1–48. (Available at http://www-odp.tamu.edu/publications/189_SR/VOLUME/CHAPTERS/106.PDF)

Clowes, C. D. (1985), *Stoveracysta*, a new gonlyaulacacean dinoflagellate genus from the upper Eocene and lower Oligocene of New Zealand, *Palynology*, *9*, 27–35.

Cookson, I. C., and A. Eisenack (1965), Microplankton from the Browns Creek Clays, SW Victoria, *Proc. R. Soc. Victoria*, *79*, 119–137.

Crouch, E. M., and C. J. Hollis (1996), Paleogene palynomorph and radiolarian biostratigraphy of DSDP Leg 29, Sites 280 and 281, South Tasman Rise, *Inst. Geol. Nucl. Sci. Rep.*, *19*, 1–46.

Dale, B. (1996), Dinoflagellate cyst ecology: Modelling and geological applications, in *Palynology: Principles and Applications*, edited by J. Jansonius and D. C. McGregor, pp. 1249–1275, Am. Assoc. of Stratigr. Palynol. Found., Salt Lake City, Utah.

Desikachary, T. V., and P. M. Sreelatha (1989), *Oamaru Diatoms*, *Bibliotheca Diatomologica, Band 19*, 475 pp., Cramer, Berlin.

Edwards, A. R. (1991), The Oamaru Diatomite, *Geol. Surv. of N. Z. Paleontol. Bull. 64*, 260 pp., Lower Hutt, N. Z.

Exon, N. F., et al. (2001), *Proceedings of the Ocean Drilling Program*, *Initial Reports*, vol. 189, Ocean Drill. Program, College Station, Tex.

Fenner, J. (1984), Eocene-Oligocene planktic diatom stratigraphy in the low latitudes and the high southern latitudes, *Micropaleontology*, *30*, 319–342.

Fenner, J., and N. Mikkelsen (1990), Eocene-Oligocene diatoms in the western Indian Ocean: Taxonomy, stratigraphy, and paleoecology, *Proc. Ocean Drill. Program Sci. Results*, *115*, 433–463.

Firth, J. V. (1996), Upper middle Eocene to Oligocene dinoflagellate biostratigraphy and assemblage variations in Hole 913B, Greenland Sea, *Proc. Ocean Drill. Program Sci. Results*, *151*, 203–242.

Florindo, F., S. M. Bohaty, P. S. Erwin, C. Richter, A. P. Roberts, P. A. Whalen, and J. M. Whitehead (2003), Magnetobiostratigraphic chronology and palaeoenvironmental history of Cenozoic sequences from ODP Sites 1165 and 1166, Prydz Bay, Antarctica, *Palaeogeogr. Palaeoclimatol. Palaeoecol.*, *198*, 69–100.

Fuller, M., and Y. Touchard (2004), On the magnetostratigraphy of the East Tasman Plateau, timing of the opening of the Tasmanian Gateway and paleoenvironmental changes: Results from ODP Leg 189 Site 1172, in *The Cenozoic Southern Ocean: Tectonics, Sedimentation and Climate Change Between Australia and Antarctica*, *Geophys. Monogr. Ser.*, vol. 151, edited by N. F. Exon, J. P. Kennett, and M. J. Malone, AGU, Washington, D. C., in press.

Gersonde, R., V. Spiess, J. A. Flores, R. Hagan, and G. Kuhn (1998), The sediments of Gunnerus Ridge and Kainan Maru Seamount (Indian sector of the Southern Ocean), *Deep Sea Res.*, *45*, 1515–1540.

Gombos, A. M. (1983), Middle Eocene diatoms from the South Atlantic, *Initial Rep. Deep Sea Drill. Project*, *71*, 565–581.

Gombos, A. M., and P. Ciesielski (1983), Late Eocene to early Miocene diatoms from the southwest Atlantic, *Initial Rep. Deep Sea Drill. Project*, *71*, 583–634.

Goodman, D. K., and L. N. Ford (1983), Preliminary dinoflagellate biostratigraphy for the Middle Eocene to Lower Oligocene from southwest Atlantic Ocean, *Initial Rep. Deep Sea Drill. Project*, *71*, 859–877.

Guerstein, G. R., J. O. Chiesa, M. V. Guler, and H. H. Camacho (2002), Bioestratigrafia basada en quistes de dinoflagelados de la Formacion Cabo Pena (Eoceno terminal-Oligoceno temprano), Tierra del Fuego, Argentina, *Rev. Esp. Micropaleontol.*, *34*, 105–116.

Hajós, M. (1976), Upper Eocene and lower Oligocene Diatomacae, Archaeomonadaceae and Silicoflagellatae in southwestern Pacific sediments, DSDP Leg 29, *Initial Rep. Deep Sea Drill. Project*, *35*, 817–883.

Hannah, M. J., and J. I. Raine (Eds.) (1997), Southern Ocean late Cretaceous/early Cenozoic biostratrigraphic datums: A report of the Southern Ocean paleontology workshop, *Sci. Rep.*, *4*, 33 pp., Inst. of Geol. and Nucl. Sci., Lower Hutt, N. Z.

Harwood, D. M. (1986), Diatoms, in *Antarctic Cenozoic History From the MSSTS-1 Drillhole, McMurdo Sound*, *DSIR Bull.*, vol. 237, edited by P. J. Barrett, pp. 69–107, Manaaki Whenua Press, Lincoln, N. Z.

Harwood, D. M. (1989), Siliceous microfossils, in *Antarctic Cenozoic History From the CIROS-1 Drillhole, McMurdo Sound*, *DSIR Bull.*, vol. 245, edited by P. J. Barrett, pp. 67–97, Manaaki Whenua Press, Lincoln, N. Z.

Harwood, D. M. (1991), Cenozoic diatom biogeography in the southern high latitudes: Inferred biogeographical barriers and progressive endemism, in *Proceedings of the Fifth International Symposium on Antarctic Earth Sciences*,

edited by M. R. A. Thompson, J. A. Crame, and J. W. Thomson, pp. 667–673, Sci. Committ. on Antarct. Res., Scott Polar Res. Inst., Cambridge, UK, 23–28 Aug.

Harwood, D. M., and S. M. Bohaty (2000), Marine diatom assemblages from Eocene and younger erratics, McMurdo Sound, Antarctica, in *Paleobiology and Paleoenvironments of Eocene Rocks, McMurdo Sound, East Antarctica*, *Antarct. Res. Ser.*, vol. 76, edited by J. D. Stilwell and R. M. Feldmann, pp. 73–98, AGU, Washington, D. C.

Harwood, D. M., and S. M. Bohaty (2001), Early Oligocene siliceous microfossil biostratigraphy of Cape Roberts Project Core CRP-3, Victoria Land Basin, Antarctica, *Terra Antarct.*, *8*, 315–338.

Harwood, D. M., and T. Maruyama (1992), Middle Eocene to Pleistocene diatom biostratigraphy of Southern Ocean sediments from the Kerguelen Plateau, Leg 120, *Proc. Ocean Drill. Program Sci. Results*, *120*, 683–734.

Harwood, D. M., P. J. Barrett, T. A. Edwards, H. J. Rieck, and P.-N. Webb (1989), Biostratigraphy and chronology, in *Antarctic Cenozoic History From the CIROS-1 Drillhole, McMurdo Sound*, *DSIR Bull.*, vol. 245, edited by P. J. Barrett, pp. 231–239, Manaaki Whenua Press, Lincoln, N. Z.

Harwood, D. M., et al. (1992), Neogene integrated magnetobiostratigraphy of the Southern Kerguelen Plateau, ODP Leg 120, *Proc. Ocean Drill. Program Sci. Results*, *120*, 1031–1052.

Haskell, T. R., and G. J. Wilson (1975), Palynology of Sites 280–284, DSDP Leg 29, off southeastern Australia and western New Zealand, *Initial Rep. Deep Sea Drill. Project*, *29*, 723–741.

Holmes, R. W., and A. L. Brigger (1977), The morphology and occurrence of Entogonia from an Eocene locality in the Indian Ocean, in *Nova Hedwigia, Fourth Symposium on Recent and Fossil Marine Diatoms*, edited by R. Simonsen, pp. 215–241, Lubrecht and Cramer, Stüttgart.

Huber, M., H. Brinkhuis, C. E. Stickley, K. Döös, A. Sluijs, J. Warnaar, S. A. Schellenberg, and G. L. Williams (2004), Eocene circulation of the Southern Ocean: Was Antarctica kept warm by subtropical waters?, *Paleoceanography*, PA4016, doi:10.1029/2004PA001014, in press.

Kemp, E. M. (1975), Palynology of Leg 28 drill sites, Deep Sea Drilling Project, *Initial Rep. Deep Sea Drill. Project*, *28*, 599–623.

Kennett, J. P., et al. (Eds.) (1975), *Initial Reports of the Deep Sea Drilling Project*, vol. 29, 1197 pp., U.S. Govt. Print. Off., Washington, D. C.

Lawver, L. A., and L. M. Gahagan (2003), Evolution of Cenozoic seaways in the circum-Antarctic region, *Palaeogeogr. Palaeoclimatol. Palaeoecol.*, *198*, 11–37.

Lear, C. H., H. Elderfield, and P. A. Wilson (2000), Cenozoic deep-sea temperatures and global ice volumes from Mg/Ca in benthic foraminiferal calcite, *Science*, *287*, 269–272.

Levy, R. H., and D. M. Harwood (2000), Tertiary marine palynomorphs from the McMurdo Sound erratics, Antarctica, in *Paleobiology and Paleoenvironments of Eocene Rocks, McMurdo Sound, East Antarctica*, *Antarct. Res. Ser.*, vol. 76, edited by J. D. Stilwell and R. M. Feldmann, pp. 183–242, AGU, Washington, D. C.

Mao, S., and B. A. R. Mohr (1995), Middle Eocene dinocysts from Bruce Bank (Scotia Sea, Antarctica) and their paleoenvironmental and paleogeographic implications, *Rev. Palaeobot. Palynol.*, *86*, 235–263.

Miller, K. G., J. D. Wright, and R. G. Fairbanks (1991), Unlocking the ice house: Oligocene-Miocene oxygen isotopes, eustacy and margin erosion, *J. Geophys. Res.*, *96*, 6829–6848.

Mohr, B. A. R. (1990), Eocene and Oligocene sporomorphs and dinoflagellate cysts from Leg 113 drill sites, Weddell Sea, Antarctica, *Proc. Ocean Drill. Program Sci. Results*, *113*, 595–612.

Murphy, M. G., and J. P. Kennett (1986), Development of latitudinal thermal gradients during the Oligocene: Oxygen isotope evidence from the southwest Pacific, *Initial Rep. Deep Sea Drill. Project*, *90*, 1347–1360.

Oberhänsli, H., J. McKenzie, M. Toumarkine, and H. Weissert (1984), A paleoclimatic and paleoceanographic record of the Paleogene in the central South Atlantic (Leg 73, Sites 522, 523, and 524), *Initial Rep. Deep Sea Drill. Project*, *73*, 737–747.

Quilty, P. G., E. M. Truswell, P. E. O'Brien, and F. Taylor (1999), Paleocene-Eocene biostratigraphy and palaeoenvironment of east Antarctica: New data from the Mac. Robertson Shelf and western parts of Prydz Bay, *AGSO J. Austr. Geol. Geophys.*, *17*, 133–143.

Ramsay, A. T. S., and J. G. Baldauf (1999), *A Reassessment of the Southern Ocean Biochronology*, *Geol. Soc. Mem.*, vol. 18, 122 pp., Geol. Soc., London.

Roberts, A. P., S. J. Bicknell, J. Byatt, S. M. Bohaty, F. Florindo, and D. M. Harwood (2003), Magnetostratigraphic calibration of Southern Ocean diatom datums from the Eocene-Oligocene of Kerguelen Plateau (Ocean Drilling Program Sites 744 and 748), *Palaeogeogr. Palaeoclimatol. Palaeoecol.*, *198*, 145–168.

Rochon, A., A. de Vernal, J. L. Turon, J. Mathiessen, and M. J. Head (Eds.) (1999), *Distribution of Recent Dinoflagellate Cysts in Surface Sediments From the North Atlantic Ocean and Adjacent Seas in Relation to Sea-Surface Parameters*, *AASP Contrib. Ser.*, vol. 35, Am. Assoc. of Stratigr. Palynol. Found., Salt Lake City, Utah.

Röhl, U., H. Brinkhuis, C. E. Stickley, M. Fuller, S. A. Schellenberg, G. Wefer, and G. L. Williams (2004), Sea level and astronomically induced environmental changes in middle and late Eocene sediments from the East Tasman Plateau, in *The Cenozoic Southern Ocean: Tectonics, Sedimentation and Climate Change Between Australia and Antarctica*, *Geophys. Monogr. Ser.*, vol. 151, edited by N. F. Exon, J. P. Kennett, and M. J. Malone, AGU, Washington, D. C., in press.

Schellenberg, S. A., H. Brinkhuis, C. E. Stickley, M. Fuller, F. T. Kyte, and G. L. Williams (2004), The Cretaceous/Paleogene transition on the East Tasman Plateau, southwestern Pacific, in *The Cenozoic Southern Ocean: Tectonics, Sedimentation and Climate Change Between Australia and Antarctica*, *Geophys. Monogr. Ser.*, vol. 151, edited by N. F. Exon, J. P. Kennett, and M. J. Malone, AGU, Washington, D. C., in press.

Schrader, H. J., and R. Gersonde (1978), Diatoms and silicoflagellates, in *Micropaleontological Counting Methods and Techniques: An Exercise of an Eight Metres Section of the Lower Pliocene of Cap Rossello, Sicily*, *Utrecht Micropaleontol. Bull.*, vol. 17, edited by W. J. Zachariasse et al., pp. 129–176, Utrecht Univ., Utrecht.

Shackleton, N. J., M. A. Hall, D. Pate, L. Meynadier, and P. Valet (1993), High-resolution stable isotope stratigraphy from bulk sediment, *Paleoceanography*, *8*, 141–148.

Shafik, S., and M. Idnurm (1997), Calcareous microplankton and polarity reversal stratigraphies of the upper Eocene Browns Creek Clay in the Otway Basin, southeast Australia: Matching the evidence, *Austr. J. Earth Sci.*, *44*, 77–86.

Shipboard Scientific Party (1999), Site 1123: North Chatham Drift—A 20-Ma record of the Pacific Deep Western Boundary Current, *Proc. Ocean Drill. Project Initial Rep.*, *181*, 1–112.

Shipboard Scientific Party (2001a), Site 1172, *Proc. Ocean Drill. Project Initial Rep.*, *189*, 1–149.

Shipboard Scientific Party (2001b), Explanatory notes, *Proc. Ocean Drill. Project Initial Rep.*, *189*, 1–59.

Shipboard Scientific Party (2001c), Site 1170, *Proc. Ocean Drill. Project Initial Rep.*, *189*, 1–167.

Shipboard Scientific Party (2001d), Site 1171, *Proc. Ocean Drill. Project, Initial Rep.*, *189*, 1–176.

Shipboard Scientific Party (2001e), Leg 189 Summary, *Proc. Ocean Drill. Project, Initial Rep.*, *189*, 1–98.

Sluijs, A., H. Brinkhuis, C. E. Stickley, J. Warnaar, G. L. Williams, and M. Fuller (2003), Dinoflagellate cysts from the Eocene–Oligocene transition in the Southern Ocean: Results from ODP Leg 189, *Proc. Ocean Drill. Program Sci. Results*, *189*, 1–42. (Available at http://www-odp.tamu. edu/publications/189_SR/VOLUME/CHAPTERS/104.PDF)

Stickley, C. E., et al. (2004), Late Cretaceous-Quaternary biomagnetostratigraphy of ODP Sites 1168, 1170, 1171 and 1172, Tasmanian Gateway, *Proc. Ocean Drill. Program Sci. Results*, *189*, 1–57. (Available at http://www-odp.tamu.edu/publications/189_SR/VOLUME/CHAPTERS/111.PDF)

Stover, L. E. (1975), Observations on some Australian Eocene dinoflagellates, *Geosci. Man. Proc. 6th Annu. Meet. Am. Assoc. Stratigr. Palynol.*, *11*, 35–45.

Stover, L. E., et al. (1996), Mesozoic-Tertiary dinoflagellates, acritarchs and prasinophytes, in *Palynology: Principles and Applications*, edited by J. Jansonius and D. C. McGregor, chap. 19, pp. 641–750, Am. Assoc. of Stratigr. Palynol. Found., Salt Lake City, Utah.

Truswell, E. M. (1997), Palynomorph assemblages from marine Eocene sediments on the west Tasmanian continental margin and the South Tasman Rise, *Austr. J. Earth Sci.*, *4*, 633–654.

Williams, G. L., , J. K. Lentin, and R. A. Fensome (Eds.) (1998), *The Lentin and Williams Index of Fossil Dinoflagellates 1998 Edition*, *Contrib. Ser.*, vol. 34, 178 pp., Am. Assoc. of Stratigr. Palynol. Found., Salt Lake City, Utah.

Wilpshaar, M., A. Santarelli, H. Brinkhuis, and H. Visscher (1996), Dinoflagellate cysts and mid-Oligocene chronostratigraphy in the central Mediterranean region, *J. Geol. Soc. London*, *153*, 553–561.

Wilson, G. J. (1967), Some new species of Lower Tertiary dinoflagellates from McMurdo Sound, Antarctica, *N. Z. J. Botany*, *5*, 57–83.

Wrenn, J. H., and S. W. Beckmann (1982), Maceral, total organic carbon, and palynological analyses of Ross Ice Shelf Project Site J-9 cores, *Science*, *216*, 187–189.

Wrenn, J. H., and G. F. Hart (1988), Paleogene dinoflagellate cyst biostratigraphy of Seymour Island, Antarctica, *Geol. Soc. Am. Mem.*, *169*, 321–447.

Wrenn, J. H., M. J. Hannah, and J. I. Raine (1998), Diversity and palaeoenvironmental significance of Late Cainozoic marine palynomorphs from the CRP-1 core, Ross Sea, Antarctica, *Terra Antarct.*, *5*, 553–570.

Zachos, J. C., T. M. Quinn, and K. A. Salamy (1996), High-resolution (10^4 years) deep-sea foraminiferal stable isotope records at the Eocene-Oligocene climate transition, *Paleoceanography*, *11*, 251–266.

Zachos, J. C., M. Pagani, L. Sloan, E. Thomas, and K. Billups (2001), Trends, rhythms, and aberrations in global climate 65 Ma to present, *Science*, *292*, 686–693.

H. Brinkhuis, A. Sluijs, and J. Warnaar, Laboratory of Palaeobotany and Palynology, Utrecht University, Utrecht N-3584, Netherlands.

M. Fuller, HIGP-SOEST, University of Hawaii, Honolulu, HI 96822, USA.

M. Grauert, Department of Geography, University of Copenhagen, Copenhagen DK-1350, Denmark.

M. Huber, Earth and Atmospheric Science, Purdue University, West Lafayette, IN 47907, USA.

U. Röhl, Research Center for Ocean Margins (RCOM), Department of Geosciences, Bremen University, Bremen D-330440, Germany.

S. A. Schellenberg, Department of Geological Sciences, San Diego State University, San Diego, CA 92182, USA.

C. E. Stickley, School of Earth, Ocean and Planetary Sciences, Cardiff University, Cardiff CF10 3YE, UK. (cathy@earth.cf.ac.uk)

G. L. Williams, Geological Survey of Canada (Atlantic), Bedford Institute of Oceanography, Dartmouth, NS B2Y 4A2, Canada.